fermentation

MDPI

Article

(S)-2-Hydroxyisovalerate Production from D-Xylose with CO-Converting *Clostridium ragsdalei*

Irina Schwarz [1], Markus Rupp [1], Oliver Frank [2], Andreas Daschner [2] and Dirk Weuster-Botz [1,*]

[1] Chair of Biochemical Engineering, Technical University of Munich, Boltzmannstr. 15, 85748 Garching, Germany; irina.schwarz@tum.de (I.S.)
[2] Chair of Food Chemistry and Molecular Sensory Science, Technical University of Munich, Lise-Meitner-Str. 34, 85354 Freising, Germany; oliver.frank@tum.de (O.F.); andreas.daschner@tum.de (A.D.)
* Correspondence: dirk.weuster-botz@tum.de; Tel.: +49-89-289-15712

Abstract: *Clostridium ragsdalei* was found to produce (S)-2-hydroxyisovalerate (2-HIV) as a novel product in addition to acetate, ethanol, and D-2,3-butanediol in heterotrophic (D-xylose), autotrophic (CO), and mixotrophic (D-xylose + CO) conditions. Mixotrophic batch processes in stirred-tank bioreactors with continuous gassing resulted in improved production of this alpha-hydroxy acid compared to batch processes solely with either D-xylose or CO. The maximal CO uptake rate was considerably reduced in mixotrophic compared to autotrophic processes, resulting in a concomitant decreased total CO_2 production. Simultaneous conversion of 9.5 g L^{-1} D-xylose and 320 mmol CO enabled the production of 1.8 g L^{-1} 2-HIV in addition to 1.1 g L^{-1} D-2,3-butanediol, 2.0 g L^{-1} ethanol, and 1.8 g L^{-1} acetate. With reduced initial D-xylose (3.1 g L^{-1}), L-valine production started when D-xylose was depleted, reaching a maximum of 0.4 g L^{-1} L-valine. Using L-arabinose or D-glucose instead of D-xylose in mixotrophic batch processes reduced the 2-HIV production by *C. ragsdalei*. Considerable amounts of *meso*-2,3-butanediol (0.9–1.3 g L^{-1}) were produced instead, which was not observed with D-xylose. The monomer 2-HIV can form polyesters that make the molecule attractive for application as bioplastic (polyhydroxyalkanoates) or new composite material.

Keywords: 2-hydroxyisovalerate; 2-hydroxy-3-methylbutyric acid; polyhydroxyalkanoates; PHA; *Clostridium ragsdalei*; syngas fermentation; D-xylose; *meso*-2,3-butanediol

Citation: Schwarz, I.; Rupp, M.; Frank, O.; Daschner, A.; Weuster-Botz, D. (S)-2-Hydroxyisovalerate Production from D-Xylose with CO-Converting *Clostridium ragsdalei*. *Fermentation* **2024**, *10*, 546. https://doi.org/10.3390/fermentation10110546

Academic Editor: Le Zhang

Received: 18 September 2024
Revised: 18 October 2024
Accepted: 19 October 2024
Published: 25 October 2024

1. Introduction

The synthesis of value-added molecules from fossil resources comes along with the production of greenhouse gases [1]. Especially, the use of microorganisms as whole-cell biocatalysts is an alternative to the classical chemical synthesis processes of producing fine chemicals, pharmaceuticals, platform chemicals, or biofuels from renewable resources [2,3]. The vast variety of microorganisms existing in nature offers very diverse characteristics based on their genetic features. Depending on the target product, the production strain has to be decided, and an optimal process design is needed. The standard whole-cell biocatalysts are aerobic microorganisms using respiration for energy supply, such as *Escherichia coli* [4,5], *Corynebacterium glutamicum* [6,7] or *Pseudomonas putida* [8], with the exception of ethanol fermentation by yeasts. Moreover, *Cupriavidus necator* is prominent in regards to polyhydroxyalkanoate (PHA) production [9,10]. Less thoroughly explored are strictly anaerobic and acetogenic microorganisms since their growth requirements entail complicated laboratory handling for a long time. Nonetheless, the ability of acetogenic bacteria to fix gaseous substrates into alcohols is a remarkable characteristic that can be beneficial for the chemical industry, and a few acetogens, such as *Acetobacterium woodii* [11], *Clostridium ljungdahlii* [12], and *Clostridium autoethanogenum* [13], have already been well investigated. The mutants of *C. autoethanogenum* are used nowadays for the industrial-scale production of ethanol [14,15].

In this study, the Gram-positive bacterium *Clostridium ragsdalei* [16], an acetogen that is genetically close to *C. autoethanogenum* and *C. ljungdahlii* [17], attracted our attention, as it is less researched than the other two but is also able to produce ethanol and D-2,3-butanediol as platform chemicals, using CO, CO_2, and H_2 as gaseous substrates [18]. In regards to its autotrophic growth behavior, results had shown that sulfide supply improved the alcohol production in general [19], and a specific dissolved CO concentration, which was dependent on the applied CO partial pressure and the bioreactor power input, optimized the alcohol production [20]. Using a trickle-bed reactor was also beneficial for the ethanol production by *C. ragsdalei* [21].

Moreover, the bacterium is able to convert various acids into their corresponding alcohols [22]. Many studies about *C. ragsdalei* focused on optimizing the fermentation medium to improve the alcohol production. For example, adding biochar to the medium that was derived from biowastes, such as poultry litter [23] or switchgrass and red cedar [24], provided many nutrients that increased the ethanol yield. Replacing yeast extract with corn steep liquor was also possible and increased the final ethanol titer [25,26]. Varying the trace metal concentration in the medium can control the product distribution as well [27]. In the respective study, the researchers found that increasing the Ni^{2+}, Zn^{2+}, SeO_4^-, and WO_4^- content in ATCC medium increased the ethanol production and improved the growth of *C. ragsdalei*.

For carbon fixation during autotrophic growth with CO or CO_2/H_2, *C. ragsdalei* uses the linear reductive acetyl-CoA pathway (the Wood–Ljungdahl Pathway, WLP) [17]. Within the methyl branch, the carbon in the CO_2 is sequentially reduced to a methyl group (bound to tetrahydrofolate) and then combined with a carbonyl group together with Coenzyme A to form the central intermediate acetyl-CoA. The carbon can enter the pathway as CO_2 or CO because the carbon monoxide dehydrogenase enables the conversion of CO to CO_2 or vice versa. Biomass, acetate, ethanol, and D-2,3-butanediol are synthesized as the main products from acetyl-CoA. For a more detailed description and illustration of the WLP, the reader is referred to the literature [28–31].

The WLP is very energy efficient in regards to carbon fixation, as it only requires one ATP that is recovered by acetate production from acetyl-CoA [32]. To produce biomass and building blocks, the cell is dependent on further ATP production through an energy conservation system. Here, H_2 and CO play a major role as electron donors in producing reduced ferredoxin, which is the key reducing equivalent in acetogenic bacteria for ATP production and redox balance [28,33]. The electrons in the reduced ferredoxin are transferred to another electron acceptor in parallel to the establishment of an ion gradient across the membrane, and the energy for ATP synthesis by an ATPase is drawn either from a proton or a Na^+ gradient (chemiosmotic ion gradient-driven phosphorylation [28]). Two different energy conservation systems have been found: the Ech-complex [34,35] and the Rnf-complex [36]. The latter one was also found in *C. ragsdalei* [17]. CO-converting bacteria, including *C. ragsdalei*, directly use the energy from CO to CO_2 oxidation to reduce ferredoxin by the carbon monoxide dehydrogenase, making CO a more favored substrate over CO_2/H_2 from a thermodynamic point of view [32,33].

Apart from the autotrophic properties, *C. ragsdalei* is known to use heterotrophic carbon sources as well, such as xylose, fructose, sucrose, and glucose [16]. In general, hexoses are metabolized via glycolysis to pyruvate that is converted to acetyl-CoA by a puruvate:ferredoxine oxidoreductase (PFOR) [37]. Pentoses are transformed to fructose-6-phosphate and glyceraldehyde-3-phosphate within the pentose phosphate pathway to be channeled into glycolysis [37]. During this oxidative part of the metabolism, $NAD(P)^+$ and ferredoxin are reduced. These must be regenerated in the reductive part of the metabolism. For comparison, aerobes use the electron transport chain to finally transfer the electrons to oxygen. Acetogenic bacteria use the WLP to reduce CO_2 (or CO) to acetate. Regarding sole autotrophic growth, H_2 or CO are oxidized to generate reducing equivalents, such as NADH and reduced ferredoxin [28]. Here, different enzyme complexes with electron-bifurcating functions allow the coupling of endergonic and exergonic reduction reactions [38], such

as the hydrogenase HydABC in *A. woodii* [39], the HytA-E in *C. autoethanogenum* [40], or the Nfn complex in *C. ljungdahlii* or *C. autoethanogenum* [41,42]. The carbon fixation through the WLP is the reductive part, and the production of acetate, ethanol, and D-2,3-butanediol consumes reducing equivalents as well [43]. Considering the carbon source, organotrophic or lithotrophic, the ATP yield is different [44]. However, balancing all the components involved in redox homeostasis is still difficult since the enzymatic constitution for some reactions of the WLP or redox metabolism is still not unraveled, especially for *C. ragsdalei*. The reliable redox potential of the involved ferredoxins remains unknown [28]. For *A. woodii*, *C. ljungdahlii*, and *C. autoethanogenum*, many findings exist, and calculations in regards to the ATP yield were performed assuming the participation of certain redox mediators [28,33,41]. In summary, the redox metabolism is very important for acetogenic bacteria as it determines the product spectrum, which is also dependent on the reduction degree of the used carbon source [43,45].

The metabolic conversion of organotrophic substrates releases CO_2. Therefore, the idea of coupling heterotrophic growth with CO_2 fixation through acetogenic bacteria under mixotrophic conditions is reasonable in terms of decreasing CO_2 emissions and creating a circular carbon economy [46]. From another perspective, the additional consumption of energy-rich sugar sources could be advantageous since autotrophic growth occurs under energy-limited conditions [28]. However, the WLP offers a very efficient redox and energy economy that might allow an optimized mixotrophic process design using acetogenic bacteria to channel the carbon from heterotrophic and lithotrophic sources into target products without (or reduced) CO_2 production [46].

Mixotrophic fermentation using sugars and synthesis gas components (CO, H_2, and CO_2) is less investigated, but studies have already revealed that regulation within the cell can hamper the co-utilization of various substrates, and these mechanisms differ significantly between acetogenic bacteria. *A. woodii* is able to consume fructose, CO_2, and H_2 in parallel [47], and the increased amount of fixed carbon was reflected by higher biomass and acetate production. Using the same cultivation conditions without CO_2 in the gas phase, growth was disabled, indicating an inhibition by H_2. In the same study, *Clostridium aceticum* was also inhibited by H_2, but that was pH dependent, and no significant gas consumption was observed during fructose usage, a sign for a downregulated WLP. Moreover, *C. ljungdahlii* was shown to consume fructose, CO_2, and H_2 simultaneously, and the respective study gave insights to its mixotrophic behavior [48]. On the one hand, the utilization of the autotrophic substrates by *C. ljungdahlii* was still dominant. On the other hand, the Nfn complex was not important for the redox economy under mixotrophic conditions. However, studies on the CO conversion in parallel to the fructose consumption are missing. Further aspects were evaluated in investigations with *Clostridium carboxidivorans* [49], where heterotrophic chemostats (glucose) were fed with different gas mixtures. Similar to *C. aceticum* [47], H_2 feeding did not induce its consumption, but CO supply, either as part of synthesis gas or purely, enabled its parallel utilization to glucose. Interestingly, the carbon efficiency was lower when CO and glucose were consumed together in comparison to heterotrophic growth, indicating that the CO to CO_2 reduction served partly to produce reduced ferredoxin.

Looking one step further, mixotrophic process designs using sugars and (waste) synthesis gas from the gasification of biomass [50] or electrolytic techniques [20,51] as substrates for acetogenic bacteria offer an opportunity for carbon-efficient production processes. Plant residues as natural carbon storage consist of (ligno)cellulosic polymers that can be degraded to their monomeric sugars. These serve as substrates for yeasts to be converted to ethanol [52]. In general, the released sugars can be used for any fermentation process. Here, one critical issue remains: the pretreatment of the plant biomass (mechanical, heat, or enzymatic) to achieve high monomeric sugar yields without inhibitors for microbial growth [53]. The above-mentioned studies focused on the mixotrophic consumption of hexoses. Nevertheless, pentoses, such as D-xylose or L-arabinose, are building blocks of hemicellulose, and their fraction in residual plant waste varies depending on the plant source.

Not every microorganism is able to use pentoses, but their conversion is essential for good carbon efficiency when using plant-based biomass. Mann et al. [54] demonstrated that simultaneous conversion of CO and D-xylose by wild-type *C. autoethanogenum* was beneficial, and in a recent study, *C. autoethanogenum* converted CO and L-arabinose to 9.5 g L^{-1} ethanol, 2.2 g L^{-1} D-2,3-butanediol, and 1 g L^{-1} *meso*-2,3-butanediol in mixotrophic batch processes [55]. Another possibility is to engineer bacteria or yeasts towards pentose utilization to enable parallel consumption with hexoses without catabolite repression [56–58]. Examples of *Saccharomyces cerevisiae* used to produce isobutanol, 2,3-butanediol, and 3-hydroxypropionic acid from D-xylose were reviewed by Lee et al. [59].

Since the isolation of *C. ragsdalei*, it is known that this bacterium can convert D-xylose [16], but no studies on defined mixotrophic processes exist. To gain more insights, this study aimed to focus on the behavior of *C. ragsdalei* under mixotrophic conditions using D-xylose as a heterotrophic substrate and an artificial synthesis gas mixture as an autotrophic source in batch-operated stirred tank bioreactors with continuous gassing. In the first mixotrophic batch process, the product 2-hydroxyisovalerate (2-HIV) was newly discovered to be synthesized in considerable amounts besides acetate, ethanol, and D-2,3-butanediol. Therefore, reaction engineering studies were conducted with *C. ragsdalei* in controlled batch processes using different initial D-xylose concentrations with a defined synthesis gas mixture containing CO, CO_2, and H_2 to investigate the product distributions. Differences between autotrophic, heterotrophic, and mixotrophic growth in regards to the product distribution were analyzed eventually. In addition, mixotrophic batch processes with L-arabinose and D-glucose were performed for comparison.

2. Materials and Methods

2.1. Identification of 2-HIV as a Novel Product of C. ragsdalei

The unknown product found on the HPLC chromatogram (see Figure 1) was isolated according to the following procedure: The final fermentation sample (10 mL) from the mixotrophic process using an initial D-xylose concentration of 9.6 g L^{-1} was lyophilized (Lyophilizer Alpha 1–2 LD plus, Martin Christ Gefriertrocknungsanlagen GmbH, Osterode am Harz, Germany), resuspended in 1 mL of reverse osmosis (RO) water, and filtered (0.2 µm size exclusion). The concentrated sample (100 µL) was loaded on a carbohydrate-analysis column (Aminex HPX-87H, Biorad, Munich, Germany), installed in a HPLC (LC2030C-Plus, Shimadzu, Kyoto, Japan). Formic acid (10 mM) was used as the mobile phase, and the analytes of the sample were separated isocratically on the column (T = 60 °C) at a volume flow of 0.6 mL min^{-1}. Following this, the fraction of the unknown by-product was collected manually. The procedure was performed several times until around 30 mL fraction was collected. The fraction was lyophilized again and resuspended in 1 mL of MS-grade water. Finally, the pure and concentrated sample could be analyzed using NMR spectroscopy (see Figure 1), and the molecular weight was verified using mass spectroscopy.

All one- (1H, 13C) and two-dimensional NMR measurements (1H, 1H correlation spectroscopy (COSY); 1H, 13C heteronuclear single-quantum coherence (HSQC); 1H, 13C hetero-nuclear multiple-bond correlation (HMBC)) for structure verification were conducted at 300.15 K on an Avance NEO 500 MHz System (Bruker, Rheinstetten, Germany) equipped with a cryoprobe (CP 2.1 TCI). Data acquisition and analysis were performed using TopSpin 4.1.1 software (Bruker, Rheinstetten, Germany). 1H NMR (500 MHz, methanol-d4, H,H COSY) δ (ppm): 0.84 [d, 3H, *J* = 6.9 Hz, H-C(4a)], 1.0 [d, 3H, *J* = 6.9 Hz, H-C(4b)], 2.05 [m, 1H, H-C(3)], 3.77 [d, 1H, *J* = 3.3 Hz, H-C(2)]. 13C NMR (125 MHz, methanol-d4, HSQC, HMBC) δ (ppm): 15.2 [CH3, C(4a)], 18.8 [CH3, C(4b)], 31.6 [CH, C(3)], 76.8 [CH, C(2)], 179.9 [C, C(1)]. For the determination of specific optical rotation, the polarimeter Jasco P-2000 Digital Polarimeter (Jasco Deutschland GmbH, Pfungstadt, Germany) with a 5 cm cuvette was employed. The aperture was set to 1.8 mm.

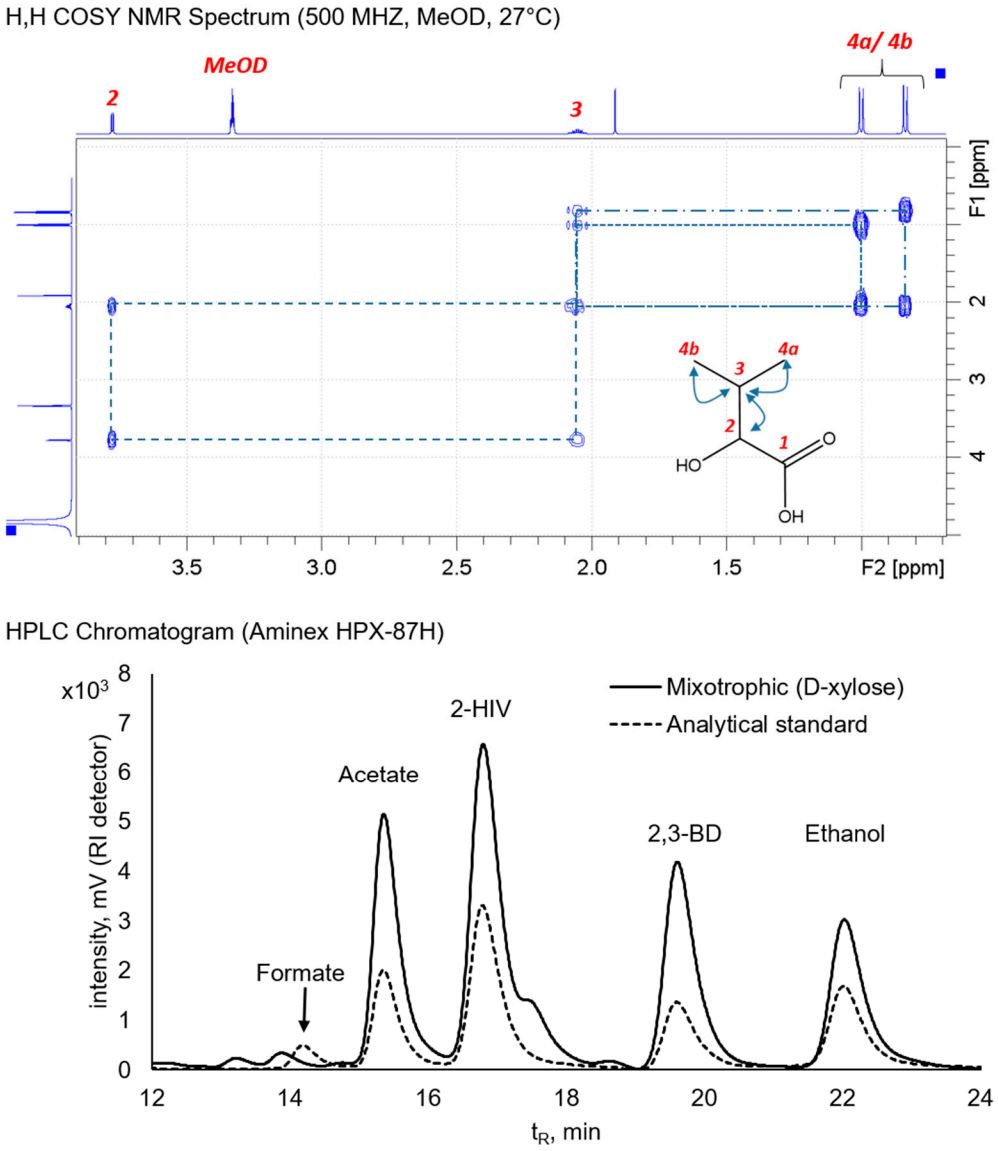

Figure 1. H,H COSY NMR spectrum of 2-hydroxyisovalerate (2-HIV; 2-hydroxy-3-methylbutyric acid), isolated and purified from the fermentation broth, and the HPLC Chromatogram (Aminex-87H analysis column, Biorad, Munich, Germany) of a filtered fermentation sample with a maximal 2-HIV concentration. Details about collecting 2-HIV from the fermentation broth are described in the methods Section 2.1. The analyte concentrations in the HPLC standard were 0.4 g L^{-1} sodium formate, 2 g L^{-1} sodium acetate trihydrate, 1 g L^{-1} 2-HIV, 0.4 g L^{-1} D-2,3-butanediol (2,3-BD), and 1 g L^{-1} ethanol. Equal sample amounts were loaded on the HPLC analysis column.

Samples were dissolved in deionized water and measured at room temperature (22 °C). The isolated compound showed the same optical activity/direction of polarization as the reference compound (2S)-2-hydroxy-3-methylbutyric acid.

2.2. Microorganisms, Media, and Inoculum Preparation

C. ragsdalei was ordered from the German Collection of Microorganism and Cell Cultures GmbH (DSM No. 15248, DSMZ GmbH, Braunschweig, Germany). The freeze-dried sample was used to inoculate anaerobic cultivation medium according to the procedure recommended by DSMZ GmbH. The anaerobically grown culture was aliquoted to Hungate tubes using 10% (*v*/*v*) glycerol or 5% (*v*/*v*) DSMO, and the tubes were stored at −80 °C. The fermentation medium for inoculum preparation and the batch processes was composed according to Doll et al. [60]. The pre-cultivation medium was prepared with

15 g L^{-1} 2-(N-morpholino)ethanesulfonic acid (MES) as a buffer in a 2 L batch, boiled for 20 min, purged with N_2 for 20 min, and was then aliquoted to 0.5 L anaerobic bottles in an anaerobic glove box. Afterward, the anaerobic bottles were sterilized by autoclaving. Cysteine-hydrochloride as a reducing agent and D-xylose stocks were prepared with anaerobic water and autoclaved as well.

The two-step inoculum preparation has already been described [20]. For inoculation and to achieve an initial cell dry weight concentration of 0.030–0.035 g L^{-1} in the bioreactor, the required volume of the second autotrophic pre-culture (gas mixture: 1.2 bar CO, 0.4 bar CO_2, and 0.4 bar H_2) was centrifuged and resuspended in 10 mL of anaerobic PBS buffer.

2.3. Batch Processes in a Continuously Gassed Standard Stirred Tank Bioreactor

All mixotrophic batch processes with D-xylose were conducted in a 2 L standard stirred tank bioreactor (Labfors, Infors AG, Bottmingen, Switzerland) with 1 L working volume. The bioreactor was fully controlled (pH 5.5, T = 32 °C, n = 1200 min^{-1}, volumetric power input P V^{-1} = 11.8 W L^{-1}) and equipped with baffles and two Rushton turbines. The pH was measured with a sterilizable probe (405-DPAS-SC-K8s/120, Mettler Toledo, Giesen, Germany). The vessel was continuously gassed with a defined synthesis gas mixture (200 mbar CO, 200 mbar CO_2, 200 mbar H_2, and 400 mbar N_2) using a gas volume flow of 5 NL h^{-1} (ambient pressure). The gas volume flows were controlled either by a compact module (WMR, Westphal Mess-und Regeltechnik, Offenbach, Germany) or by four independent mass flow controllers (F-201CV-500 RGD-33-V, Bronkhorst High Tech B.V., Ruurlo, The Netherlands), depending on the used bioreactor station.

The stirred tank bioreactor was autoclaved with RO water. Afterwards, the reactor was connected to the control station, and 5 NL h^{-1} N_2 purging was started. The water was replaced by an autoclaved fermentation medium (without vitamins) using aseptic methods. The sterile filtrated vitamin solution was added via a septum, and the vessel was anaerobized for at least one hour with N_2. Overnight, the bioreactor was conditioned with the desired synthesis gas mixture.

Mixotrophic batch processes with L-arabinose and D-glucose were conducted in a different bioreactor using the same working volume of 1 L as before. The geometry of the other reaction vessel, a 2.4 L stainless steel stirred-tank (KLF2000, Bio-Engineering, Wald, Switzerland), differed slightly as the reactor diameter was smaller, resulting in a higher volumetric power input (P V^{-1} = 15.1 W L^{-1}). Due to excess gas supply and only small gas conversion in mixotrophic fermentations, the dissolved gas concentrations are not limiting for *C. ragsdalei* so that the different power inputs of the reactors did not affect the CO uptake rate and the bacterial growth. The stirred tank was sterilized in place with the fermentation medium (121 °C for 21 min at p_{abs} = 2.2 bar), and vitamins were added aseptically after sterilization. The same probes were used for pH and redox measurements as described before.

Prior to inoculation, 0.4 g L^{-1} L-cysteine-HCl was always added from an anaerobic stock as a reducing agent under aseptic conditions, as well as the anaerobic D-xylose, L-arabinose, or D-glucose solution for the mixotrophic batch process.

2.4. Product Quantification

Regular samples were taken in the batch processes. For calculating the cell dry weight concentration (CDW), the optical density at 600 nm was converted to CDW using a device-specific OD_{600}-CDW correlation. Concentrations of the sugar, acids, and alcohols were determined by HPLC (LC2030C-Plus, Shimadzu, Kyoto, Japan) using filtered fermentation samples (0.2 µm size exclusion). Analytes were separated on a carbohydrate-analysis column (Aminex HPX-87H, Biorad, Munich, Germany) using a constant volume flow (0.6 mL min^{-1}) of 5 mM H_2SO_4. A refractive index detector (RID-20A, Shimadzu, Kyoto, Japan) detected the analytes, and using an external standard calibration, the peak areas were converted to the respective concentration values.

L-valine was also quantified by HPLC using a different analysis method but the same instrument. Amino acids were derivatized prior to analysis that was automated by the HPLC instrument. A total of 1 µL of the filtered fermentation sample (0.2 µm size exclusion) was added to a destination vial (65.8 µL of a 40 mM bicine buffer solution (pH 10.2) containing 0.34 mM 3-mercaptopropionic acid). Next, 2 µL of an iodoacetic acid solution (3.5 mM in 40 mM bicine) and then 7 µL of an o-phthaldialdehyde solution (OPA) were added to the destination vial. The OPA solution was prepared by dissolving 100 mg OPA in 5 mL methanol and 5 mL 40 mM bicine buffer (pH 10.2), adding 65 µL 3-mercaptopropionic acid, and diluting it ten times. Between each pipetting step of the derivatization procedure, the sample was mixed 3 times using a mixing volume of 25 µL, and the reaction mixture was incubated for 1 min. Finally, 10 µL of the mixture was loaded on the analysis column (Gemini C18 column, 150 mm × 4.6 mm × 5 µm, 110 Å, Phenomenex Ltd., Aschaffenburg, Germany). The flow rate of the mobile phase was 1 mL min^{-1}, and the column temperature was controlled to 40 °C. A 20 mM NaH_2PO_4 solution was used as solvent A, and in the analysis method, a gradient was applied with solvent B (methanol/acetonitril/water = 45%/45%/10% (*v*/*v*/*v*)) according to the certain profile: 0–3 min 100% solvent A, 8.5 min 75% solvent A, 30 min 60% solvent A, 30.02 min 0% solvent A, 32 min 0% solvent A, 34 min 20% solvent A (increased flow rate to 1.2 mL min^{-1}), 38 min 100% solvent A (flow rate 1 mL min^{-1}), and 43 min 100% solvent A.

2.5. Off-Gas Analysis

A mass flow meter (F-111B-500-RGD-33-E, Bronkhorst, High Tech B.V., Ruurlo, Netherlands) measured the mass flow of the off-gas before it was analyzed online by gas chromatography (490 Micro GC or 450 Micro GC, Agilent Technologies, Waldbronn, Germany). Both micro GCs were equipped with different analysis columns. The 490 micro GC model consisted of a COX column to analyze CO, H_2, and CO_2, and the 450 micro GC had one molecular sieve 5A column to separate CO, H_2, and N_2 and a PlotPQ column to quantify CO_2. In both micro GCs, analytes were detected by thermal conductivity.

The resulting peak areas were converted to the respective gas shares using an external calibration with defined gas mixtures. If N_2 was not measured (490 micro GC), the N_2 share was calculated by subtracting the other gas shares from the absolute pressure. For each measurement, the mixing gas conversion factor was calculated to correct the off-gas mass flow. The factor considered the individual gas calibration parameters and the measured gas shares. Multiplying the measured exhaust gas volume flow by the factor, each gas volume flow (CO, H_2, CO_2, and N_2) could be calculated. The gas uptake rates were determined by subtracting the actual volume flow from the initial volume flow and conversion to [mmol L^{-1} h^{-1}]. To attain total gas consumption in mmol, the rate was integrated over time using a 10 min increment.

2.6. Carbon and Electron Recoveries

The consumed D-xylose amount and final product concentrations were converted to [mmol C L^{-1}]. Finally, total produced carbon (biomass, 2-HIV, acetate, ethanol, 2,3-butanediol, and L-valine) was related to the total consumed carbon (CO, D-xylose, and yeast extract) to determine carbon recoveries. Using the reduction degrees of the substrates and products, including H_2, the respective electron recoveries could be calculated.

3. Results

3.1. 2-HIV Production by C. ragsdalei in Autotrophic, Heterotrophic, and Mixotrophic Batch Processes with D-*Xylose*

Autotrophic batch processes have been performed previously with *C. ragsdalei*, studying the influence of pH, temperature, sulfide, and pCO on process performance [19,20]. In the HPLC chromatograms for the analysis of carbohydrates and alcohols, an unknown peak was always present in the data of the autotrophic batch processes, but with a neglectable small peak area. Performing the first mixotrophic batch process with D-xylose

and synthesis gas as substrates revealed that these conditions supported the synthesis of the so-far unknown product, identified later as 2-hydroxy-3-methylbutyric acid (or 2-hydroxyisovalerate) by NMR analysis. Polarimeter measurements with the purified molecule revealed that the (S)-enantiomer was produced by *C. ragsdalei.* In the following experiments, batch processes were conducted in a fully controlled standard stirred tank bioreactor (pH 5.5, 32 °C, and n = 1200 min^{-1}) with continuous gassing. The mixotrophic batch process using 9.5 ± 0.4 g L^{-1} D-xylose initially was then compared to the heterotrophic conditions using 4.8 or 9.2 g L^{-1} D-xylose. Moreover, the already published autotrophic reference process [20] was included, this time with four instead of two replicates, together with the final quantification of 2-HIV. The respective results are presented in Figure 2.

Mixotrophic conditions enabled the production of 2-HIV with up to 1.8 ± 0.2 g L^{-1} after a process time of 6 d. When D-xylose was depleted after 4 d, the production of 2-HIV stopped. Under autotrophic conditions at 200 mbar CO, finally 1.1 ± 0.3 g L^{-1} 2-HIV was produced by *C. ragsdalei* after 6 d. Pure heterotrophic conditions enabled the synthesis of 2-HIV as well, but the autotrophic and mixotrophic 2-HIV production started earlier. In the case of the autotrophic batch process, the end of the exponential growth phase was almost reached at a biomass concentration of around 0.4 g L^{-1} CDW when the 2-HIV synthesis started at a process time of 1.7 d. Under mixotrophic conditions, *C. ragsdalei* was still in the exponential growth phase at t = 0.8 d when 2-HIV synthesis began. Consuming 4.8 g L^{-1} D-xylose in the heterotrophic batch process, 2-HIV could be detected only in the end in tiny amounts, whereas a higher initial sugar concentration of 9.2 g L^{-1} D-xylose enabled a longer total process time and therefore a higher final 2-HIV concentration. At the time of stopping the heterotrophic process with a higher availability of D-xylose, the sugar was not completely consumed, but regarding the 2-HIV concentration at t = 4.8 d, 0.7 g L^{-1} was produced in comparison to 1.1 ± 0.3 g L^{-1}, gained from CO as a sole carbon source in the autotrophic batch process.

Product formation kinetics with regard to the other fermentation products, acetate, ethanol, and D-2,3-butanediol, exhibited several variations. The time course of the acetate concentration, both for the autotrophic and mixotrophic processes, is divided into two phases, but the phase durations differ. For the mixotrophic case, the acetate production rate is high until the end of the exponential growth phase that was reached at t = 1.5 d and then slowed down until the end of the batch process, resulting in 1.8 ± 0.7 g L^{-1} acetate. In the autotrophic batch process, acetate increased with increasing CDW concentration until the maximum was achieved at t = 3 d and stayed constant until the end of the batch process. However, the maximal acetate concentration of 2.7 ± 0.4 g L^{-1} is in the same range as the mixotrophic process, and that was also true for the final acetate concentration in the heterotrophic process.

Mixotrophic ethanol production started with a delay after 0.4 d and was synthesized up to 2.0 ± 0.8 g L^{-1} ethanol as long as D-xylose was available, similar to the production of 2-HIV. Autotrophic ethanol production was detected after 1 d, and synthesis continued for further 5 days, which was growth-decoupled, so that maximal 4.5 ± 0.4 g L^{-1} ethanol was measured. Interestingly, the ethanol production rate was similar under autotrophic and mixotrophic conditions within the exponential growth phase. During heterotrophic growth, ethanol was produced at a lower level, generally. With 4.8 g L^{-1} D-xylose, ethanol was synthesized in parallel to biomass and acetate. A higher amount of 9.8 g L^{-1} D-xylose rather served for biomass and acetate production, and at higher CDW concentrations, for the production of the longer-chained products D-2,3-butanediol and 2-HIV.

The D-2,3-butanediol production started together with the 2-HIV synthesis at t = 0.8 d in the mixotrophic process. In the end, a maximum of 1.1 ± 0.3 g L^{-1} D-2,3-butanediol was reached. D-2,3-butanediol was also synthesized continuously under autotrophic conditions, but the production started later in the end of the exponential growth phase (t = 1.5 d). Finally, 0.81 ± 0.10 g L^{-1} D-2,3-butanediol was attained by autotrophic growth and differed not significantly from the mixotrophic process.

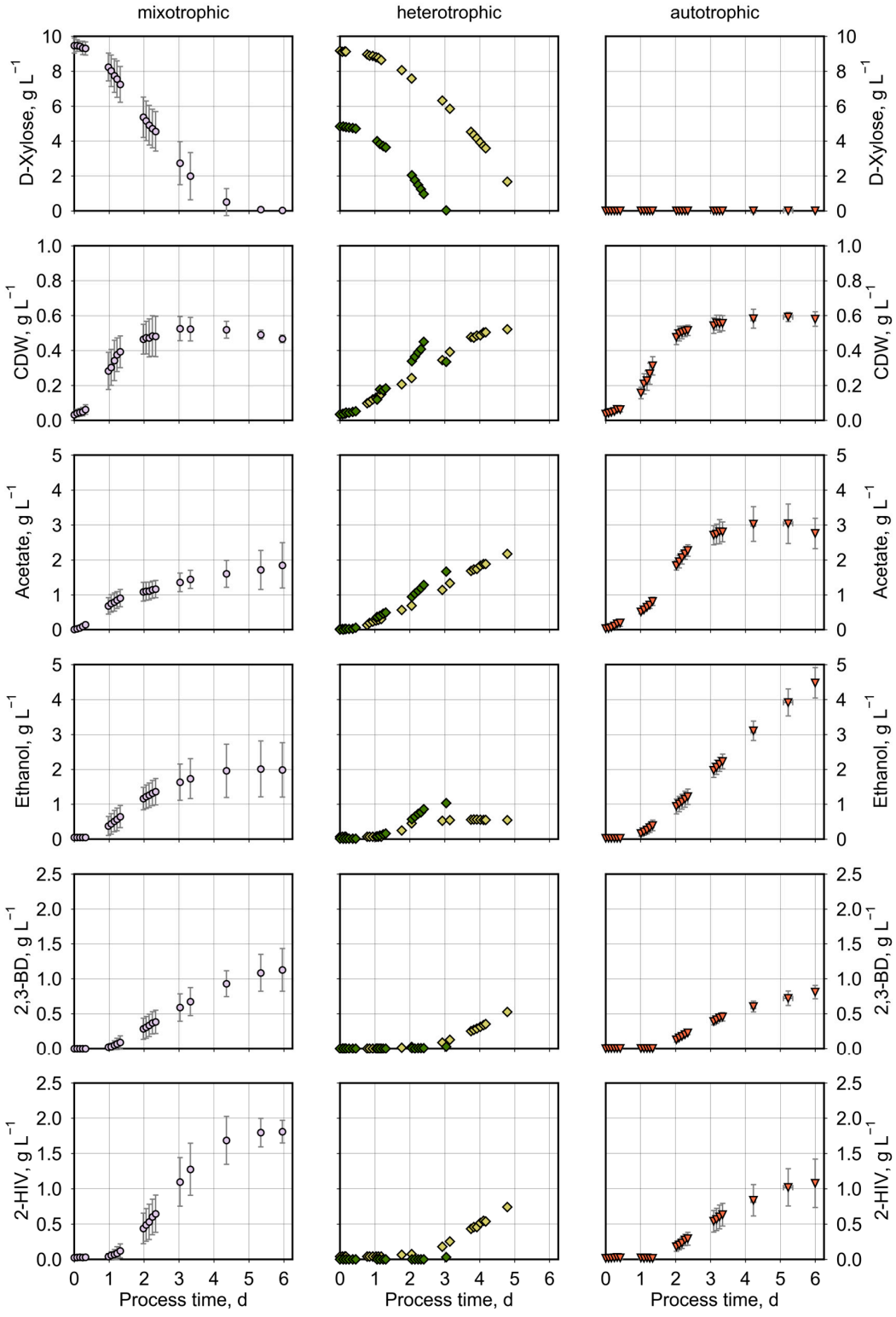

Figure 2. Product formation by *C. ragsdalei* in autotrophic, heterotrophic, and mixotrophic batch processes in stirred tank bioreactors with continuous gassing. In autotrophic and mixotrophic processes, the synthesis gas mixture was composed of 20% (*v*/*v*) CO, CO_2, and H_2 each and 40% (*v*/*v*) N_2. The heterotrophic processes were conducted with 90% (*v*/*v*) N_2 and 10% (*v*/*v*) CO_2 (V = 1 L, $F_{gas,in}$ = 5 L h^{-1}, 32 °C, pH 5.5, and n = 1200 min^{-1}). The autotrophic batch process was conducted with 4 replicates and the mixotrophic with 3 replicates.

The D-xylose consumption kinetics revealed further differences between the mixotrophic and heterotrophic growth with 9.8 g L^{-1} D-xylose. Both curves showed a sigmoidal decay behavior, but simultaneous CO consumption led to a faster D-xylose decrease. It took 4.5 d for total sugar utilization, whereas in heterotrophic growth, the residual D-xylose concentration was 3 g L^{-1} at this process time.

Moreover, the exhaust gas was analyzed online by gas chromatography, and the gas uptake rates for heterotrophic, autotrophic, and mixotrophic growth in relation to time are depicted in Figure 3.

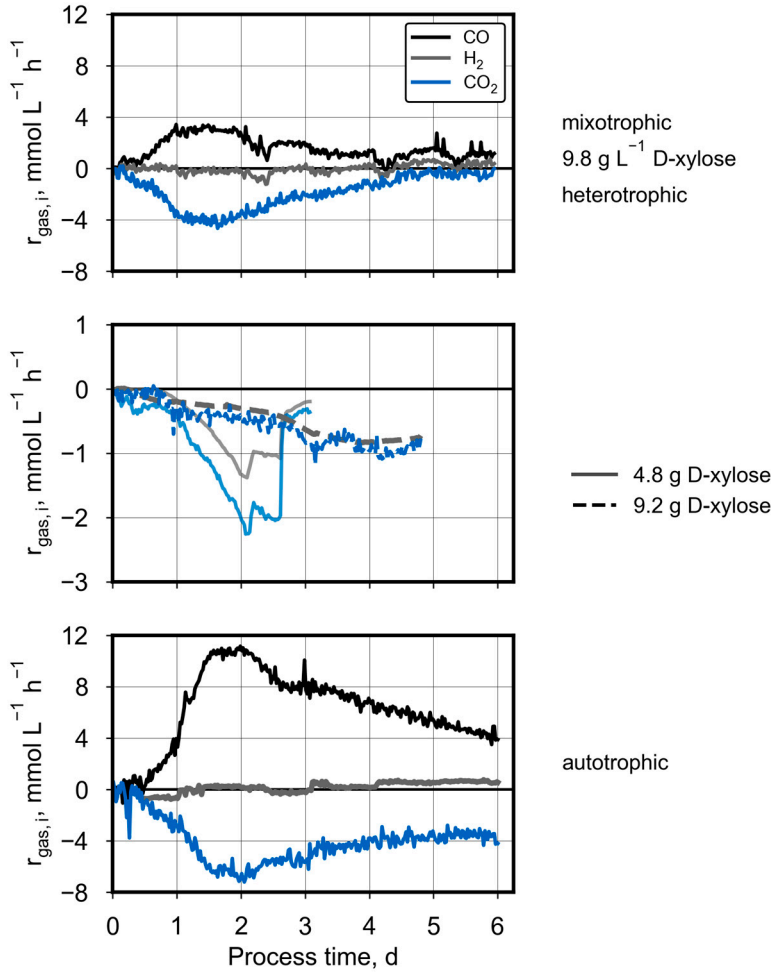

Figure 3. Gas uptake rates in autotrophic, heterotrophic (D-xylose), and mixotrophic batch processes in stirred tank bioreactors with continuous gassing. In autotrophic and mixotrophic processes, the synthesis gas mixture was composed of 20% (*v*/*v*) CO, CO_2, and H_2 each and 40% (*v*/*v*) N_2. The heterotrophic processes were conducted with 90% (*v*/*v*) N_2 and 10% (*v*/*v*) CO_2 ($F_{gas,in}$ = 5 L h^{-1}, 32 °C, pH 5.5, and n = 1200 min^{-1}). The data for the mixotrophic and autotrophic processes represent the results of one representative process with three (mixotrophic) or four (autotrophic) replicates.

The CO uptake rate was substantially reduced to 2.9 ± 1.0 mmol L^{-1} h^{-1} during mixotrophic growth, whereas an uptake rate of 13.2 ± 2.5 mmol L^{-1} h^{-1} was reached during autotrophic growth at maximal CDW concentration. That correlated with a decreased CO_2 production rate of 3.4 ± 0.5 mmol L^{-1} h^{-1} under mixotrophic conditions in comparison to 8.2 ± 0.9 mmol L^{-1} h^{-1} during growth solely using CO. Significant H_2 uptake or production was not observed.

During heterotrophic D-xylose utilization, CO_2 and H_2 were released in parallel. Due to the higher growth rate in the process using initially 4.8 g L^{-1} D-xylose, the maximal gas production rates were higher (1.4 mmol L^{-1} h^{-1} H_2 and 2.3 mmol L^{-1} h^{-1} CO_2,

respectively) than in the heterotrophic process using 9.2 g L^{-1} D-xylose. In both cases, the production rates rose until the maximal CDW concentration was achieved. In the heterotrophic process with initially 9.2 g L^{-1} D-xylose, a total production of 52 mmol H_2 and 67 mmol CO_2, respectively, was observed, whereas 4.8 g L^{-1} D-xylose resulted in a gas release of 36 mmol H_2 and 47 mmol CO_2. Sugar depletion was reflected by a rapid drop in the gas production rates when 4.8 g L^{-1} D-xylose was supplied. Using initially 9.2 g L^{-1} D-xylose, the sugar was not completely consumed after 4.8 d, and therefore, no sudden decrease in the CO_2 and H_2 production was observed.

In summary, heterotrophic (D-xylose), autotrophic, and mixotrophic batch fermentations with *C. ragsdalei* proved the production of 2-HIV. However, the product distribution differed as autotrophy supported growth-decoupled ethanol production, and mixotrophy resulted in a carbon flow towards the longer-chained product 2-HIV. Simultaneous CO and sugar conversion were observed in mixotrophic cultivations, but sugar availability reduced CO utilization.

3.2. Mixotrophic Batch Processes with Various Initial D-*Xylose Concentrations*

Using 9.5 ± 0.4 g L^{-1} D-xylose, the 2-HIV production seemed to stagnate in the stationary growth phase so that no growth-decoupled production was observed. Therefore, we assumed that a higher 2-HIV concentration cannot be achieved in our mixotrophic batch process design. Moreover, the CO consumption was significantly reduced with sugar supply. Consequently, we reduced the initial D-xylose concentration with *C. ragsdalei* to study the effect on the product distribution and the CO consumption. Following this, initial D-xylose concentrations of 7.3 g L^{-1}, 4.7 ± 0.1 g L^{-1}, and 3.1 ± 0.4 g L^{-1} were tested (see Figure 4).

Reducing the initially supplied D-xylose concentration, decreased the final 2-HIV concentration to 1.1 g L^{-1}, 1.2 ± 0.1 g L^{-1}, and 1.3 ± 0.4 g L^{-1}, respectively (Figure 4). In the mixotrophic batch processes with 7.3 g L^{-1} and 9.5 ± 0.4 g L^{-1} D-xylose, the 2-HIV production ceased with sugar depletion. On supplying 4.7 ± 0.1 g L^{-1} or 3.1 ± 0.4 g L^{-1} D-xylose, growth-decoupled 2-HIV synthesis was observed.

Biomass, acetate, ethanol, and D-2,3-butanediol formations were very similar for all mixotrophic processes shown in Figure 4. Independent of the initial sugar concentrations, 2–3 g L^{-1} ethanol, 0.55 g L^{-1} CDW at the maximum, and 0.6–1.3 g L^{-1} D-2,3-butanediol were measured. In contrast, the supply of 3.1 ± 0.4 g L^{-1} D-xylose increased the maximal CDW concentration to 0.63 ± 0.1 g L^{-1} and the final acetate concentration to 3.3 ± 0.8 g L^{-1}. Comparing specific product yields between the different mixotrophic processes, the ethanol yield was not dependent on the sugar concentration, as 4.0 ± 0.6, 4.4 ± 1.1, 3.8, and 3.7 ± 1.2 $g_{Ethanol}$ $g_{CDW}{}^{-1}$ were determined with 3.1 ± 0.4, 4.7 ± 0.1, 7.3, and 9.5 ± 0.4 g L^{-1} D-xylose, respectively. A small increase in the 2,3-butanediol yield (1.1 ± 0.4, 1.1 ± 0.2, 1.5, and 2.1 ± 0.8 $g_{2,3BD}$ $g_{CDW}{}^{-1}$) was observed with the highest D-xylose supply, but the effect was not substantial. For 2-HIV, the trend was significant.

Since L-valine differs from 2-HIV by the presence of an amino group instead of the 2-hydroxy group of 2-HIV, we searched for L-valine in the fermentation broth of *C. ragsdalei*. For the mixotrophic process conducted with initial 4.7 ± 0.1 g L^{-1} D-xylose, L-valine could be quantified only for two replicates. On adding less than 9.5 ± 0.4 g L^{-1} D-xylose, L-valine production was detected in mixotrophic processes. The less sugar was supplied, the earlier L-valine synthesis started and the higher its final concentration was. Using 3.1 ± 0.4 g L^{-1} D-xylose, up to 0.42 ± 0.17 g L^{-1} L-valine was produced until the end of the process.

As shown before, a high sugar supply (>4.7 g L^{-1}) under mixotrophic conditions led to a reduced CO uptake compared to the autotrophic batch process. It was evident that the higher the initial D-xylose concentration, the lower the maximal CO uptake rate.

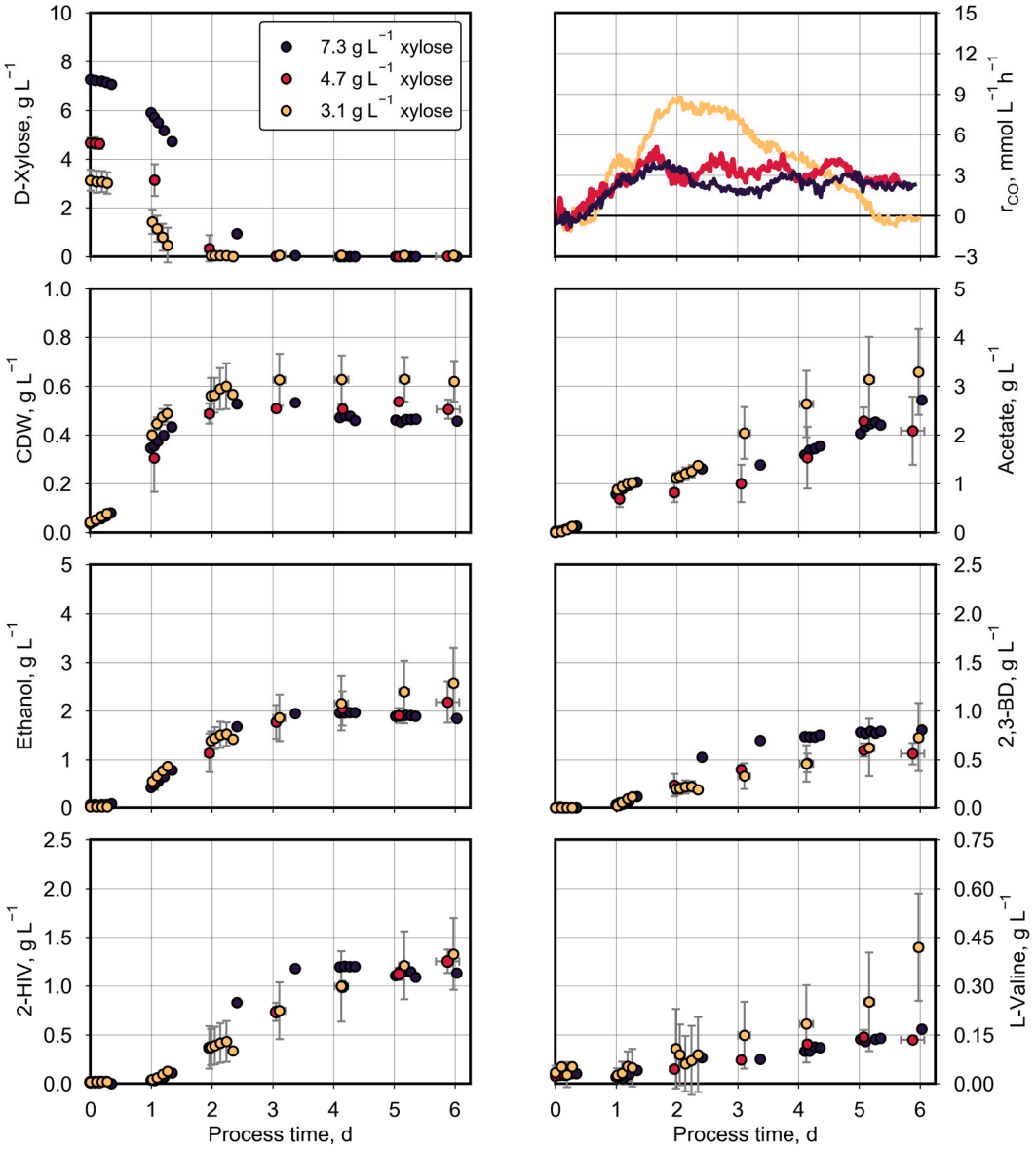

Figure 4. Product formation by *C. ragsdalei* in mixotrophic batch processes in stirred tank bioreactors with continuous gassing applying various initial D-xylose concentrations and a defined synthesis gas mixture. The synthesis gas was composed of 20% (*v*/*v*) CO, CO_2, and H_2 each, and 40% (*v*/*v*) N_2 ($F_{gas,in}$ = 5 L h^{-1}, 32 °C, pH 5.5, and n = 1200 min^{-1}). The mean values with standard deviations derive from three replicates for mixotrophic processes with 4.7 ± 0.1 g L^{-1} and 3.1 ± 0.4 g L^{-1} D-xylose. L-Valine quantification for the process with 4.7 ± 0.1 g L^{-1} was performed only for two replicates.

3.3. Mixotrophic Batch Processes with D-*Glucose and* L-*Arabinose*

Growth and product formation by *C. ragsdalei* under mixotrophic conditions were also tested with different sugars, D-glucose and L-arabinose, and compared to the mixotrophic process using D-xylose (see Figure 5).

Utilizing 9.6 g L^{-1} D-glucose or 8.8 g L^{-1} L-arabinose did not support the 2-HIV production to the same extent as 9.5 ± 0.4 g L^{-1} D-xylose, as only 0.3 and 0.9 g L^{-1} 2-HIV were measured at the end with the respective sugars as further carbon sources. However, other differences were observed in regard to growth, CO conversion, and product formation.

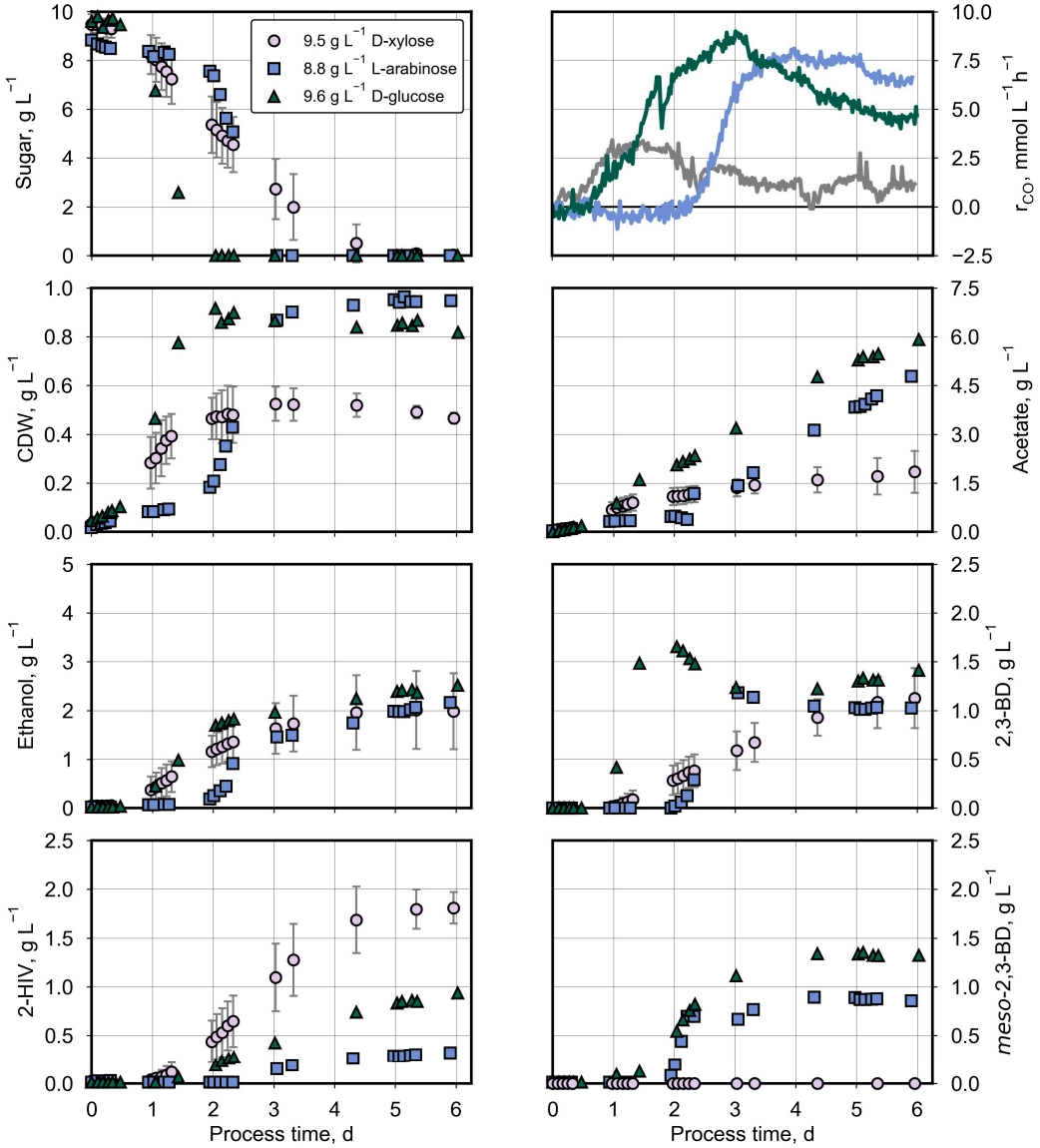

Figure 5. Product formation by *C. ragsdalei* in mixotrophic batch processes in stirred tank bioreactors with continuous gassing using different sugars, D-glucose and L-arabinose, and a defined synthesis gas mixture. The synthesis gas was composed of 20% (*v*/*v*) CO, CO_2, and H_2 each and 40% (*v*/*v*) N_2 ($F_{gas,in}$ = 5 L h^{-1}, 32 °C, pH 5.5, and n = 1200 min^{-1}).

Conversion of L-arabinose revealed a biphasic growth curve. First, the CDW concentration increased slightly (t = 0–0.8 d), then stagnated for almost one day, and then rapid growth occurred. A reversed course was observed for the sugar consumption. The maximal CDW concentration was increased by 1.8 times to 0.94 g L^{-1} in comparison to 0.52 ± 0.07 g L^{-1} using D-xylose. On applying D-glucose as a carbon source, the sugar was consumed immediately, different to L-arabinose, and faster, different to D-xylose. The maximal CDW concentration was similar to the mixotrophic process with L-arabinose but was reached almost one day earlier.

In contrast to the mixotrophic process using D-xylose, the L-arabinose and D-glucose consumption enabled the production of *meso*-2,3-butanediol. Fast D-glucose utilization resulted in the strong synthesis of D-2,3-butanediol up to 1.6 g L^{-1} initially. Afterward, at t = 1.5 d, its concentration decreased, but the production of the *meso*-2,3-butanediol diastereomer started. In the end, the presence of 1.4 g L^{-1} D-2,3-butanediol and 1.3 g L^{-1} *meso*-2,3-butanediol was determined in the mixotrophic process with D-glucose. Fast L-arabinose

conversion after 1.75 d of process time initiated the D-2,3-butanediol production as well, but the synthesis of the *meso* diastereomer started rather simultaneously. Eventually, 1.0 g L^{-1} D-2,3-butanediol and 0.8 g L^{-1} *meso*-2,3-butanediol were quantified, which is less than in the process with L-arabinose.

D-glucose and L-arabinose were converted in parallel to CO. A higher CDW concentration resulted in a higher maximal CO uptake rate in comparison to the mixotrophic process with D-xylose. The maximal CO uptake rate reached similar levels in the mixotrophic processes with D-glucose and L-arabinose.

3.4. Carbon Balances and Electron Balances

Carbon and electron balances were calculated for all batch processes of *C. ragsdalei* with continuous gassing until a process time of 100 h (4.2 d), except for the heterotrophic process with 4.8 g L^{-1} D-xylose (shorter total process time). The data are presented in Tables 1 and 2. Carbon and electron balances were closed to 92–105% (C-balance) and 89–110% (electron balance) within the estimation error, except for the mixotrophic process with L-arabinose, where the electron balance could not be closedfor unknown reasons.

Table 1. Carbon balances and electron recoveries in autotrophic and heterotrophic batch processes. The balances were calculated for a process time of 0–4.2 d, except for the heterotrophic process using 4.8 g L^{-1} D-xylose (shorter total process time of 3 d). For the electron recovery, H_2 uptake or production was included.

		Autotrophic (4 Replicates)	**Heterotrophic**	
Initial D-xylose, g L^{-1}		**0**	**4.8**	**9.2 ***
Substrates, mmol C	D-xylose	0	160	184
	CO	818 ± 124	0	0
	YE + L-cystein-HCl	9	9	9
Products, mmol C	Biomass	18 ± 1	11	16
	2-HIV	36 ± 10	1	23
	Ethanol	134 ± 14	43	24
	2,3-BD	28 ± 5	1	16
	Acetate	99 ± 15	57	63
	CO_2	525 ± 28	47	50
CO_2/total C consumed, %		62 ± 2	28	26
C-recovery, %		101 ± 3	98	98
Electron-recovery, %		99 ± 11	98	103

* 5.5 g L^{-1} were consumed.

CO utilization was substantially reduced from 818 ± 124 mmol CO in the autotrophic process (see Table 1) to 229 ± 40 mmol C under mixotrophic conditions when 9.5 ± 0.4 g L^{-1} D-xylose was supplied (see Table 2). Consequently, the CO_2 production was reduced to 189 ± 34 mmol C in the mixotrophic batch processes compared to 525 ± 28 mmol C in the autotrophic processes. Significant H_2 uptake or production was not observed.

The ratio of totally produced CO_2 per total carbon consumed (CO, xylose, carbon in yeast extract (YE), and 0.4 g L^{-1} cysteine-HCl) was calculated for the autotrophic and all mixotrophic fermentations (Tables 1 and 2), and the data are visualized in Figure 6A. The relative CO_2 release decreased with increasing D-xylose consumption in the autotrophic (62 ± 2%) and mixotrophic batch processes (down to 41 ± 3%).

Table 2. Carbon balances and electron recoveries in mixotrophic batch processes using L-arabinose, D-glucose, and D-xylose. The balances were calculated for a process time of 0–4.2 d. For the electron recovery, H_2 uptake or production was included.

		L-Arabinose	D-Glucose	D-Xylose (3 Replicates)	D-Xylose (3 Replicates)		D-Xylose (3 Replicates)
Initial Sugar, g L^{-1}		**8.8**	**9.6**	**3.1 ± 0.4**	**4.7 ± 0.1**	**7.3**	**9.5 ± 0.4**
Substrates, mmol C	Sugar	293	384	104 ± 14	156 ± 7	242	229 ± 40
	CO	520	527	515 ± 158	269 ± 9	210	153 ± 30
	YE + L-cystein-HCl	9	9	9	9	9	9
Products, mmol C	Biomass	29	27	20 ± 3	16 ± 1	15	17 ± 1
	2-HIV	11	31	43 ± 15	41 ± 1	50	70 ± 14
	Ethanol	76	97	95 ±26	89 ± 15	85	85 ± 33
	2,3-BD	47	59	21 ± 10	22 ± 5	32	41 ± 7
	meso-2,3-BD	12	45	0	0	0	0
	L-valine	n.a.	n.a.	8 ± 5	4–6	4	0
	Acetate	104	159	89 ± 24	52 ± 21	56	53 ± 12
	CO_2	260	539	323 ± 65	221 ± 11	197	189 ± 34
CO_2/total C consumed, %		46	59	52 ± 4	51 ± 3	43	41 ± 3
C-recovery, %		96	105	96 ± 6	102 ± 4	96	98 ± 4
Electron-recovery, %		82	91	94 ± 3	99 ± 6	89	92 ± 4

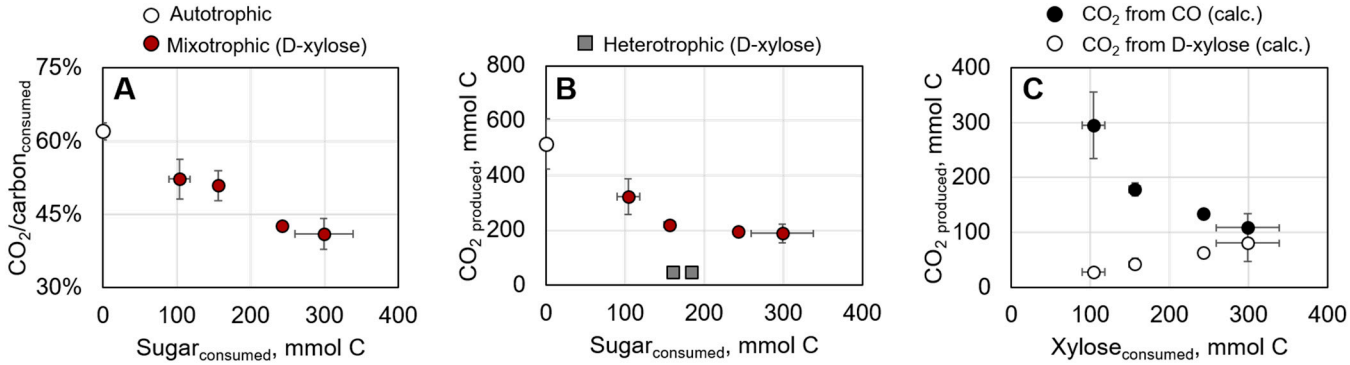

Figure 6. Comparing total CO_2 production between autotrophic, heterotrophic, and mixotrophic fermentations with *C. ragsdalei*. (**A**) Ratio of total CO_2 produced to total carbon consumed (xylose, CO, and carbon in yeast extract). (**B**) Total CO_2 produced. (**C**) Assuming that 27% of the carbon in D-xylose was released as CO_2, the CO_2 amount derived from D-xylose and the CO_2 amount derived from CO oxidation were estimated.

In addition, the total CO_2 produced (mmol C) is plotted against the utilized D-xylose (mmol C) in Figure 6B. This shows again that the mixotrophic processes with D-xylose released less CO_2 (189 ± 34 mmol C) in comparison to the autotrophic process (525 ± 28 mmol C). Whereas the released CO_2 amount in the mixotrophic batch process with L-arabinose was similar to D-xylose, the CO_2 amount released in the mixotrophic batch process with D-glucose was similar to the CO_2 amount produced autotrophically.

The heterotrophic batch processes were the lowest CO_2 producers. From 4.8 g L^{-1} D-xylose (=160 mmol C), 47 mmol CO_2 was released, which gives 28% CO_2 produced from D-xylose and the medium components. For the other heterotrophic process applying 9.2 g L^{-1} D-xylose, 26% was calculated. Using the mean value of 27% and assuming now for the mixotrophic processes with D-xylose that 27% of the carbon in D-xylose was released as CO_2, the CO_2 amount derived from CO oxidation can be estimated by subtracting the respective value from the total produced CO_2 amount (Figure 6C, black circles). The linear

correlation between the total produced CO_2 amount from D-xylose and the consumed sugar amount is obvious (Figure 6C, white circles). In consequence, the amount of CO_2 produced from CO declined with increasing initial D-xylose concentrations (Figure 6C, black diamonds).

4. Discussion

4.1. Suggesting a Route for 2-HIV Synthesis as a Novel Product of C. ragsdalei

This study demonstrated the presence of 2-HIV (2-hydroxy-3-methylbutyric acid) as a novel product of *C. ragsdalei* in addition to ethanol, D-2,3-butanediol, and acetate. Polarimeter measurements with the purified product proved the presence of (S)-enantiomer.

2-HIV possesses two chemical characteristics that make the molecule attractive for application as bioplastic. On the one hand, the two functional groups allow the formation of polyester, the so-called polyhydroxyalkanoates (PHA) [61]. On the other hand, the isopropyl group features more hydrophobicity, and it has been shown that the polyester had a higher melting temperature than polylactic acid (PLA) [62]. Moreover, the co-polymer formation of lactic acid together with 2-HIV or the co-crystallization of the corresponding pure polyesters is promising for the design of new composite materials [63–66].

2-HIV synthesis was observed in heterotrophic, autotrophic, and mixotrophic batch processes with D-xylose. Simultaneous D-xylose and CO conversion supported the synthesis of this novel by-product. Since it has the same structure as L-valine, the production through the L-valine synthesis pathway is apparent and therefore very likely (see Figure 7). Moreover, L-valine production could be detected in this study with *C. ragsdalei.*

Natural 2-HIV production was described with some subspecies of *Lactobacillus lactis* (subspec. *lactis* NCDO 2118 [67], subsp. *cremoris* MG1363 [68], and subsp. *lactis* IL1403 [69]) beside other alpha-hydroxy acids, such as 2-hydroxyisocaproate or 2-hydroxy-3-methylvalerate [70]. In these strains, similar to the D-2,3-butanediol production, the 2-HIV synthesis happens through acetolactate. However, the pathway splits then into the L-valine production and the D-2,3-butanediol production route (see Figure 7).

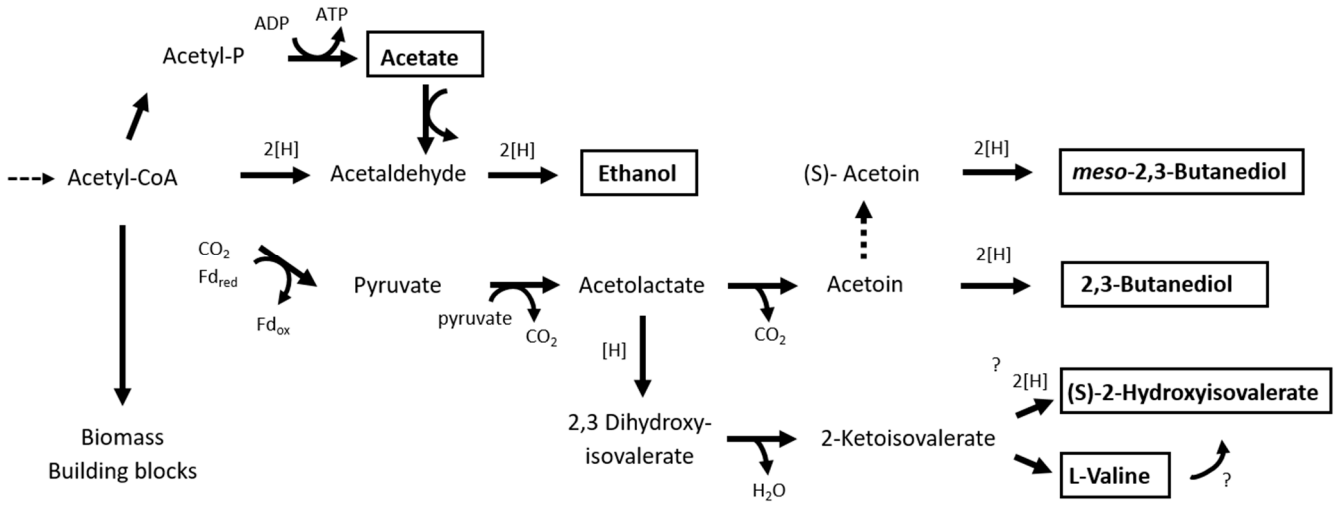

Figure 7. Proposed 2-HIV production route in *C. ragsdalei*. Synthesis of acetate, ethanol, and D-2,3-butanediol from Acetyl-CoA is illustrated according to the genetically closely related strains *C. autoethanogenum* and *C. ljungdahlii* [17,71,72].

For L-valine production, acetolactate is reduced to 2,3-dihydroxyisovalerate first and then converted to 2-ketoisovalerate. The keto group is exchanged by an amino group to form L-valine. The contig sequencing data of *C. ragsdalei* were recently annotated for a second time (genome assembly ASM167516v1, GenBank: LROS00000000.1) [17]. The genes involved in the production of L-valine were annotated in the contig sequencing data (*ilvC*: ketol acid reductoisomerase, *ilvD*: dihydroxy-acid dehydratase, and *ilvE*: branched-chain

amino acid transferases OBR95711 and OBR95035). In *L. lactis*, 2-ketoisovalerate is reduced to a hydroxy group to synthesize 2-HIV, catalyzed by a 2-hydroxyacid dehydrogenase (wrongly annotated as a 2-hydropantoate 2-reductase (PanE)) [70]. A 2-hydroxyacid dehydrogenase can be found in the sequencing data of *C. ragsdalei* as well. Nevertheless, several enzymes in *L. lactis* could catalyze the reduction of alpha-hydroxy in vitro, for instance, the L-lactate dehydrogenase [67] or the 2-hydroxyisocaproate dehydrogenase [70]. Occasionally, the reduction reaction is dependent on the branched chain. In the contig sequencing data of *C. ragsdalei*, a L-lactate dehydrogenase was annotated first but not in the second annotation data. In the HPLC chromatogram, lactate was never detected as a by-product of *C. ragsdalei*. Moreover, the already mentioned 2-hydropantoate 2-reductase (PanE) is able to catalyze the reduction of the 2-keto-group to a hydroxy group in *E. coli* [73,74]. Another group found that the ketol acid reductoisomerase (ilvC) is also active for the production of 2-HIV in engineered *Klebsiella pneumoniae* [75]. However, the genome of *C. ragsdalei* is not completely sequenced, and many genes are not annotated, suggesting that one can only speculate about the 2-HIV synthesis pathway in the acetogenic bacteria.

4.2. D-Xylose Supply in Mixotrophic Batch Processes Shifted Product Distribution from Ethanol Towards 2-HIV

Summarizing the main results, an initial high D-xylose concentration of 9.5 ± 0.4 g L^{-1} resulted in an exclusively higher 2-HIV concentration of 1.8 ± 0.2g L^{-1} in comparison to all other mixotrophic, autotrophic, and heterotrophic processes with *C. ragsdalei.* Even the autotrophic process without any sugar supply enabled the production of up to 1.1 ± 0.3 g L^{-1} 2-HIV, a final concentration comparable to the mixotrophic processes with 4.7–7.3 g L^{-1} D-xylose. The acetate and D-2,3-butanediol production did not differ between the autotrophic and mixotrophic processes, but remarkably, the growth-decoupled ethanol production was only observed when CO was the sole carbon source. In general, the CO uptake abated the more D-xylose was consumed, and less CO_2 production was measured by the exhaust gas analysis. Hence, D-xylose substituted CO as the main carbon source, but both substrates were used simultaneously.

The variations in the product spectrum, which depend on the consumed substrates, may indicate an important role of redox homeostasis in *C. ragsdalei*. During autotrophic growth, carbon is fixed through the acetyl-CoA pathway, and oxidation of electron donors (H_2, CO) is required to produce the main redox player, ferredoxin, for ATP production [28,33]. Utilizing CO as the sole carbon and electron source, the CO oxidation provides one reduced ferredoxin. Comparing the ferredoxin yield from CO to the yield possibly gained from D-xylose, one sugar molecule offers more energy, and two reduced ferredoxins are generated [28]. Therefore, the consumption of sugar as a preferred, energy-rich substrate can explain the decreased need to oxidize CO. Oppelt et al. [55] used the same fermentation medium for mixotrophic fermentations with *C. autoethanogenum*, but additional carbon from the sugar source was used for biomass production, and that could be related to higher CO consumption, completely different from *C. ragsdalei* with D-xylose. The latter strain seemed to prefer the consumption of D-xylose, but the less D-xylose was supplied, the more CO was used in total. With *C. carboxidivorans*, mixotrophic CO and glucose consumption were also beneficial for the product formation (acetate, ethanol, and 1-butanol), and an increased CO supply also enhanced CO uptake, whereas at the same time, the glucose uptake rate decreased [49].

However, mixotrophic fermentations with *C. ragsdalei* showed parallel consumption of CO and D-xylose, and the combination could have resulted in an increased pool of reduced ferredoxin and reduction equivalents. It was shown for *C. autoethanogenum* and *C. ljungdahlii* that the production of ethanol, through the aldehyde ferredoxin oxidoreductase (AOR), and the 2,3-butanediol synthesis function as electron sinks [45,76,77]. The conversion of acetate to ethanol needs one reduced ferredoxin and NADH. The production of pyruvate from acetyl-CoA by the pyruvate:ferredoxin oxidoreductase requires one reduced ferredoxin. After conversion to acetolactate and then acetoin, the final reduction to D-2,3-butanediol

requires further reduction equivalents. Mixotrophic cultivations did not support ethanol and D-2,3-butanediol production significantly, but in these processes, the 2-HIV synthesis could have assumed the respective function. Regarding the L-valine biosynthesis in Figure 7, one reduced ferredoxin is consumed for acetolactate production. Then, two reduction steps and one dehydration are required to form 2-HIV, according to the suggested pathway in the previous section. In total, more reduction equivalents are necessary. The intensified 2-HIV synthesis under high D-xylose availability supports the hypothesis of an alternative electron sink in *C. ragsdalei*. Nevertheless, the mixotrophic processes with different initial D-xylose concentrations varied in terms of growth-decoupled 2-HIV production. With higher supplied D-xylose amounts (7.3–9.5 g L^{-1}), its production stopped when the sugar was depleted, indicating an immediate termination of the carbon flux to the novel product.

On the contrary, less sugar supply enabled growth-decoupled 2-HIV production, although the sugar was already consumed completely. Additionally, growth-decoupled L-valine synthesis was observed with reduced initial D-xylose concentrations. Regarding the reduction degrees of 2-HIV and L-valine, for both, a value of 24 can be calculated if ammonium is the nitrogen source for L-valine synthesis from 2-ketoisovalerate (see Figure 7). Therefore, the regulation of their synthesis cannot be explained by redox homeostasis, and it is difficult to discuss how the ratio between 2-HIV and L-valine depends on the D-xylose concentration. Less is known about *C. ragsdalei* in regards to its genome, but a different regulation mechanism needs to be taken into account. Here, further investigations are necessary to analyze the regulation of the 2-HIV and L-valine synthesis, with the main objective of maximizing their final concentrations.

The energetic benefit from sugar conversion was also reflected by the fact that the supply of 9.5 ± 0.4 g L^{-1} D-xylose tended to reduce the acetate production in comparison to lower initial D-xylose concentrations. During autotrophic growth using the WLP pathway, one ATP is consumed that is regenerated by acetate production [28]. Sugar conversion delivers a higher yield of reduction equivalents, such as Fd_{red}, allowing a higher ATP yield and consequently decreasing the acetate production. Applying 3.1 ± 0.4 g L^{-1} D-xylose as the lowest sugar concentration in this study, the final acetate concentration was the highest of all mixotrophic processes, but similar to the final concentration in the autotrophic process. In our other study with *C. ragsdalei* [20], the autotrophic growth with reduced CO availability induced energy-limited conditions that resulted in an additional CO_2/H_2 uptake, related to a strong acetate production. In the mixotrophic process with initial 3.1 ± 0.4 g L^{-1} D-xylose, the sugar was depleted before the maximal CDW concentration was achieved so that the energy limitations were compensated by higher CO conversion and acetate production. Comparing the results to *C. autoethanogenum*, the mixotrophy of CO and D-xylose increased the ethanol and D-2,3-butanediol titers in the batch process [55], whereas for *C. ragsdalei*, 2-HIV was synthesized to a greater extent from D-xylose. Metabolization of the sugar via glycolysis yields pyruvate, and pyruvate is one precursor of 2-HIV. In this study, mixotrophy may have reduced the flux through the reductive acetyl-CoA pathway, and therefore, the acetate and the ethanol production were not supported in general, but the production of the longer-chained molecules via pyruvate instead. Regarding the biomass-specific ethanol yield produced by *C. ragsdalei*, no significant dependency on the sugar concentration was observed. The respective values for *C. autoethanogenum* in the study of Oppelt et al. [55] were 8.5, 8.3, and 9.2 $g_{Ethanol}$ $g_{CDW}{}^{-1}$ in mixotrophic processes with 19.3, 13.7, and 10.3 g L^{-1} D-xylose, showing also their independence from the initial D-xylose concentration. In contrast, the specific 2,3-butanediol yield increased with increased sugar supply for both *C. ragsdalei* (this study) and *C. autoethanogenum* [48]. However, with *C. ragsdalei*, increased 2,3-butanediol and 2-HIV yields were only observed at the highest supplied D-xylose amount (9.5 ± 0.4 g L^{-1}). We expected that with all different initial sugar concentrations (0–9.5 g L^{-1} D-xylose), a clear shift in the final product distribution from ethanol (autotrophic) to 2-HIV (mixotrophic, 9.5 ± 0.4 g L^{-1} D-xylose) would be observed with increasing initial sugar amounts. However, at lower sugar concentrations, no significant changes were observed for the ethanol, 2,3-butanediol, and 2-HIV production,

and our results showed that the total amount of consumed sugar in relation to the total consumed CO amount did not influence the product distribution. During the batch process, the available sugar concentration decreases, possibly affecting the metabolism of *C. ragsdalei*, as a shift from mixotrophic to autotrophic metabolism takes place. A continuous process design with defined sugar and CO feed rates is necessary to determine all steady state production rates under unlimited growth conditions to gain more knowledge about how the product distribution is controlled.

4.3. Conversion of D*-Glucose or* L*-Arabinose Enabled the Synthesis of Meso-2,3-Butanediol*

Similar to *C. autoethanogenum* [55], L-arabinose consumption resulted in the production of *meso*-2,3-butanediol by *C. ragsdalei*, in addition to D-2,3-butanediol, which was probably the (2R,3R)-enantiomer [18,72]. The *meso* diastereomer was produced even before the other enantiomer was detected. The acetoin can racemize to the (S)-enantiomer spontaneously, resulting in the formation of *meso*-2,3-butanediol (see Figure 7) [72].

The biphasic growth behavior with L-arabinose indicated an adaptation to L-arabinose as the sugar source, different from D-xylose and D-glucose, as they were used rather immediately. In the first pre-culture, fructose was supplied, and in the second pre-culture, only CO served as the main carbon and electron source. Therefore, for all three other sugars, the same process conditions were applied. Parallel consumption of L-arabinose with CO was also observed, however delayed, and that was distinct to *C. autoethanogenum* [55].

When rapid D-glucose consumption started, the D-2,3-butanediol production rose sharply and reached a maximum of 1.7 g L^{-1}. Small amounts of the *meso* diastereomer were also synthesized, but its strong synthesis started while the D-2,3-butanediol concentration declined and when the sugar was already consumed completely. CO was taken up simultaneously. *C. autoethanogenum* cannot utilize D-glucose, so no comparison can be drawn [13]. *C. ljungdahlii* can use D-glucose after an adaptation to the sugar source [12]. However, studies focused on the conversion of D-fructose, as it is the favored organotrophic substrate [12,44,48].

The growth of *C. ragsdalei*, both with L-arabinose and D-glucose, enabled higher biomass. Therefore, a higher CO uptake could be observed. Nevertheless, comparing their conversion to D-xylose utilization, the product spectrum shifted from 2-HIV with D-xylose to biomass, acetate, and *meso*-2,3-butanediol using L-arabinose or D-glucose.

4.4. Mixotrophy for a More Carbon-Efficient Process Design with C. ragsdalei

Reducing CO_2 emissions in terms of climate change is a current challenge, aiming to enable the carbon-efficient production of value-added molecules. Mixotrophic growth of acetogenic bacteria with organotrophic and gaseous substrates derived from waste material (plant residues or waste gases) might be an opportunity to reduce carbon release as CO_2, as it is always a by-product in either aerobic or anaerobic fermentation.

The synthesis gas mixture in this study supplied excess of the gas components (CO, H_2, and CO_2); hence, all the processes of this basic research were not carbon efficient. Large-scale applications usually aim for the utilization of all three gases by adjusting the incoming synthesis gas mixture from a previous gasification process [78]. The used gas mixture in our research was based on a previous study applying a defined gas composition, and parallel CO, CO_2, and H_2 uptake with *C. ragsdalei* was only possible under CO-limiting conditions [20]. In this study, CO was not a limiting substrate. Nevertheless, there were differences between autotrophic and mixotrophic CO conversion or CO_2 production by *C. ragsdalei*.

For example, *C. ragsdalei* released around 60% of the consumed CO as CO_2 during autotrophic growth. This value is similar to the results reported in other studies with *C. ljungdahlii* [45], *C. autoethanogenum* [79], and *C. carboxidivorans* [49]. Heterotrophic growth resulted in only 26–28% CO_2 from D-xylose. During mixotrophic growth with D-xylose, CO utilization, and consequently CO_2 evolution, was reduced, indicating that CO to CO_2 oxidation rather served for the regeneration of reduction equivalents [28,45,49]. However,

mixotrophic growth performed better than heterotrophic growth in regards to the final product concentrations, underlining again that CO is a favored substrate for *C. ragsdalei*, especially as an electron source. Moreover, mixotrophy with D-xylose outcompeted the autotrophic growth with better carbon efficiency and proved potential for future process designs with *C. ragsdalei.* Since low CO conversion was sufficient for improved growth and product formation in comparison to the heterotrophic conditions, lower CO partial pressures should be tested in further studies.

5. Conclusions

Depending on the acetogenic bacterium used, many differences are observed in organotrophic or lithotrophic substrate utilization. The types of carbon or electron source and the products with different degrees of reduction can both influence the total product distribution, and that is very individual for each acetogen, obviously.

For *C. ragsdalei*, a novel product 2-HIV was found, with putative applications as a monomer for bioplastics or novel composite material. Mixotrophic cultivations with high initial D-xylose concentration demonstrated intense production of 2-HIV in comparison to heterotrophic or autotrophic growth. Sugar consumption and less CO utilization resulted in a decreased release of carbon as CO_2, making the mixotrophic process design attractive for climate-friendly and sustainable production of value-added molecules, such as 2-HIV. Moreover, the utilization of D-glucose and L-arabinose showed the production of *meso*-2,3-butanediol.

Author Contributions: Conceptualization, I.S. and D.W.-B.; methodology—processes, I.S.; methodology—2-HIV identification, O.F. and A.D.; investigation, I.S. and M.R.; writing—original draft preparation, I.S.; writing—review and editing, D.W.-B.; visualization, I.S.; supervision, project administration, and funding acquisition, D.W.-B. All authors have read and agreed to the published version of the manuscript.

Funding: This research was funded by the priority program "eBiotech" (SPP2240) by the German Research Foundation DFG (WE2715/17-1/2).

Institutional Review Board Statement: Not applicable.

Informed Consent Statement: Not applicable.

Data Availability Statement: All relevant data are presented in the article. Quantification of H_2 was necessary for electron balances, but the data are not shown in this study since no significant H_2 consumption or production was observed.

Acknowledgments: The German Research Foundation is gratefully acknowledged for funding, as are our project partners in the "eBiotech" priority program: Tim-Patrick Fellinger, Asad Mehmood, and Arielle Rieck from the Federal Institute of Material Research and Testing (BAM, Berlin). Additionally, we want to thank the TUM Graduate School for the support of Irina Schwarz.

Conflicts of Interest: The authors declare no conflicts of interest.

References

1. Gabrielli, P.; Rosa, L.; Gazzani, M.; Meys, R.; Bardow, A.; Mazzotti, M.; Sansavini, G. Net-zero emissions chemical industry in a world of limited resources. *One Earth* **2023**, *6*, 682–704. [CrossRef]
2. Vanholme, B.; Desmet, T.; Ronsse, F.; Rabaey, K.; van Breusegem, F.; de Mey, M.; Soetaert, W.; Boerjan, W. Towards a carbon-negative sustainable bio-based economy. *Front. Plant Sci.* **2013**, *4*, 174. [CrossRef] [PubMed]
3. Tylecote, A. Biotechnology as a new techno-economic paradigm that will help drive the world economy and mitigate climate change. *Res. Policy* **2019**, *48*, 858–868. [CrossRef]
4. Huang, C.-J.; Lin, H.; Yang, X. Industrial production of recombinant therapeutics in *Escherichia coli* and its recent advancements. *J. Ind. Microbiol. Biotechnol.* **2012**, *39*, 383–399. [CrossRef]
5. Scheper, T.; Babel, W.; Blanch, H.W.; Endo, I.; Enfors, S.-O.; Fiechter, A.; Hoare, M.; Mattiasson, B.; Sahm, H.; Schügerl, K.; et al. *Microbial Production of l-Amino Acids*; Springer: Berlin/Heidelberg, Germany, 2003; ISBN 978-3-540-43383-5.
6. Becker, J.; Wittmann, C. Industrial Microorganisms: *Corynebacterium glutamicum*. In *Industrial Biotechnology: Microorganisms*; Wiley-VCH: Hoboken, NJ, USA, 2016; pp. 183–220.

7. Inui, M.; Toyoda, K. *Corynebacterium Glutamicum*; Springer International Publishing: Cham, Switzerland, 2020; ISBN 978-3-030-39266-6.
8. Weimer, A.; Kohlstedt, M.; Volke, D.C.; Nikel, P.I.; Wittmann, C. Industrial biotechnology of *Pseudomonas putida*: Advances and prospects. *Appl. Microbiol. Biotechnol.* **2020**, *104*, 7745–7766. [CrossRef]
9. Morlino, M.S.; Serna García, R.; Savio, F.; Zampieri, G.; Morosinotto, T.; Treu, L.; Campanaro, S. Cupriavidus necator as a platform for polyhydroxyalkanoate production: An overview of strains, metabolism, and modeling approaches. *Biotechnol. Adv.* **2023**, *69*, 108264. [CrossRef]
10. Sohn, Y.J.; Son, J.; Jo, S.Y.; Park, S.Y.; Yoo, J.I.; Baritugo, K.-A.; Na, J.G.; Choi, J.-I.; Kim, H.T.; Joo, J.C.; et al. Chemoautotroph *Cupriavidus necator* as a potential game-changer for global warming and plastic waste problem: A review. *Bioresour. Technol.* **2021**, *340*, 125693. [CrossRef]
11. Bache, R.; Pfennig, N. Selective isolation of *Acetobacterium woodii* on methoxylated aromatic acids and determination of growth yields. *Arch. Microbiol.* **1981**, *130*, 255–261. [CrossRef]
12. Tanner, R.S.; Miller, L.M.; Yang, D. *Clostridium ljungdahlii* sp. nov., an acetogenic species in clostridial rRNA homology group I. *Int. J. Syst. Bacteriol.* **1993**, *43*, 232–236. [CrossRef]
13. Abrini, J.; Naveau, H.; Nyns, E.-J. *Clostridium autoethanogenum*, sp. nov., an anaerobic bacterium that produces ethanol from carbon monoxide. *Arch. Microbiol.* **1994**, *161*, 345–351. [CrossRef]
14. Mihalcea, C.; Burton, F.; Conrado, R.; Simpson, S. R&D&I and Industry Examples: LanzaTech's Gas Fermentation. In *CO_2 and CO as Feedstock. Circular Economy and Sustainability*; Springer: Cham, Switzerland, 2023; pp. 333–343.
15. Liew, F.E.; Nogle, R.; Abdalla, T.; Rasor, B.J.; Canter, C.; Jensen, R.O.; Wang, L.; Strutz, J.; Chirania, P.; Tissera, S.d.; et al. Carbon-negative production of acetone and isopropanol by gas fermentation at industrial pilot scale. *Nat. Biotechnol.* **2022**, *40*, 335–344. [CrossRef] [PubMed]
16. Huhnke, R.L.; Lewis, R.S.; Tanner, R.S. Isolation and Characterization of Novel Clostridial Species. U.S. Patent 7704723B2, 31 August 2006.
17. Bengelsdorf, F.R.; Poehlein, A.; Linder, S.; Erz, C.; Hummel, T.; Hoffmeister, S.; Daniel, R.; Dürre, P. Industrial acetogenic biocatalysts: A comparative metabolic and genomic analysis. *Front. Microbiol.* **2016**, *7*, 1036. [CrossRef] [PubMed]
18. Köpke, M.; Mihalcea, C.; Liew, F.; Tizard, J.H.; Ali, M.S.; Conolly, J.J.; Al-Sinawi, B.; Simpson, S.D. 2,3-butanediol production by acetogenic bacteria, an alternative route to chemical synthesis, using industrial waste gas. *Appl. Environ. Microbiol.* **2011**, *77*, 5467–5475. [CrossRef] [PubMed]
19. Oliveira, L.; Röhrenbach, S.; Holzmüller, V.; Weuster-Botz, D. Continuous sulfide supply enhanced autotrophic production of alcohols with *Clostridium ragsdalei*. *Bioresour. Bioprocess.* **2022**, *9*, 15. [CrossRef]
20. Schwarz, I.; Angelina, A.; Hambrock, P.; Weuster-Botz, D. Simultaneous Formate and Syngas Conversion Boosts Growth and Product Formation by *Clostridium ragsdalei*. *Molecules* **2024**, *29*, 2661. [CrossRef]
21. Devarapalli, M.; Lewis, R.; Atiyeh, H. Continuous Ethanol Production from Synthesis Gas by *Clostridium ragsdalei* in a Trickle-Bed Reactor. *Fermentation* **2017**, *3*, 23. [CrossRef]
22. Isom, C.E.; Nanny, M.A.; Tanner, R.S. Improved conversion efficiencies for n-fatty acid reduction to primary alcohols by the solventogenic acetogen "*Clostridium ragsdalei*". *J. Ind. Microbiol. Biotechnol.* **2015**, *42*, 29–38. [CrossRef]
23. Sun, X.; Atiyeh, H.K.; Zhang, H.; Tanner, R.S.; Huhnke, R.L. Enhanced ethanol production from syngas by *Clostridium ragsdalei* in continuous stirred tank reactor using medium with poultry litter biochar. *Appl. Energy* **2019**, *236*, 1269–1279. [CrossRef]
24. Sun, X.; Atiyeh, H.K.; Kumar, A.; Zhang, H. Enhanced ethanol production by *Clostridium ragsdalei* from syngas by incorporating biochar in the fermentation medium. *Bioresour. Technol.* **2018**, *247*, 291–301. [CrossRef]
25. Maddipati, P.; Atiyeh, H.K.; Bellmer, D.D.; Huhnke, R.L. Ethanol production from syngas by *Clostridium* strain P11 using corn steep liquor as a nutrient replacement to yeast extract. *Bioresour. Technol.* **2011**, *102*, 6494–6501. [CrossRef]
26. Saxena, J.; Tanner, R.S. Optimization of a corn steep medium for production of ethanol from synthesis gas fermentation by *Clostridium ragsdalei*. *World J. Microbiol. Biotechnol.* **2012**, *28*, 1553–1561. [CrossRef] [PubMed]
27. Saxena, J.; Tanner, R.S. Effect of trace metals on ethanol production from synthesis gas by the ethanologenic acetogen *Clostridium ragsdalei*. *J. Ind. Microbiol. Biotechnol.* **2011**, *38*, 513–521. [CrossRef] [PubMed]
28. Schuchmann, K.; Müller, V. Autotrophy at the thermodynamic limit of life: A model for energy conservation in acetogenic bacteria. *Nat. Rev. Microbiol.* **2014**, *12*, 809–821. [CrossRef]
29. Nitschke, W.; Russell, M.J. Beating the acetyl coenzyme A-pathway to the origin of life. *Philos. Trans. R. Soc. Lond. B Biol. Sci.* **2013**, *368*, 20120258. [CrossRef]
30. Ragsdale, S.W. Enzymology of the Wood-Ljungdahl pathway of acetogenesis. *Ann. N. Y. Acad. Sci.* **2008**, *1125*, 129–136. [CrossRef] [PubMed]
31. Küsel, K.; Drake, H.L. Acetogens. In *Encyclopedia of Geobiology*; Encyclopedia of Earth Sciences Series; Springer: Dordrecht, The Netherlands, 2011.
32. Claassens, N.J.; Cotton, C.A.R.; Kopljar, D.; Bar-Even, A. Making quantitative sense of electromicrobial production. *Nat. Catal.* **2019**, *2*, 437–447. [CrossRef]
33. Bertsch, J.; Müller, V. Bioenergetic constraints for conversion of syngas to biofuels in acetogenic bacteria. *Biotechnol. Biofuels* **2015**, *8*, 210. [CrossRef]

34. Hedderich, R.; Forzi, L. Energy-converting NiFe hydrogenases: More than just H_2 activation. *J. Mol. Microbiol. Biotechnol.* **2005**, *10*, 92–104. [CrossRef]
35. Welte, C.; Krätzer, C.; Deppenmeier, U. Involvement of Ech hydrogenase in energy conservation of *Methanosarcina mazei*. *FEBS J.* **2010**, *277*, 3396–3403. [CrossRef]
36. Tremblay, P.-L.; Zhang, T.; Dar, S.A.; Leang, C.; Lovley, D.R. The Rnf complex of *Clostridium ljungdahlii* is a proton-translocating ferredoxin:NAD+ oxidoreductase essential for autotrophic growth. *mBio* **2012**, *4*, e00406-12. [CrossRef]
37. Köpke, M.; Held, C.; Hujer, S.; Liesegang, H.; Wiezer, A.; Wollherr, A.; Ehrenreich, A.; Liebl, W.; Gottschalk, G.; Dürre, P. *Clostridium ljungdahlii* represents a microbial production platform based on syngas. *Proc. Natl. Acad. Sci. USA* **2010**, *107*, 13087–13092. [CrossRef] [PubMed]
38. Peters, J.W.; Miller, A.-F.; Jones, A.K.; King, P.W.; Adams, M.W. Electron bifurcation. *Curr. Opin. Chem. Biol.* **2016**, *31*, 146–152. [CrossRef] [PubMed]
39. Katsyv, A.; Kumar, A.; Saura, P.; Pöverlein, M.C.; Freibert, S.A.; Stripp, S.T.; Jain, S.; Gamiz-Hernandez, A.P.; Kaila, V.R.I.; Müller, V.; et al. Molecular basis of the electron bifurcation mechanism in the FeFe-hydrogenase complex HydABC. *J. Am. Chem. Soc.* **2023**, *145*, 5696–5709. [CrossRef] [PubMed]
40. Wang, S.; Huang, H.; Kahnt, J.; Mueller, A.P.; Köpke, M.; Thauer, R.K. NADP-specific electron-bifurcating FeFe-hydrogenase in a functional complex with formate dehydrogenase in *Clostridium autoethanogenum* grown on CO. *J. Bacteriol.* **2013**, *195*, 4373–4386. [CrossRef]
41. Mock, J.; Zheng, Y.; Mueller, A.P.; Ly, S.; Tran, L.; Segovia, S.; Nagaraju, S.; Köpke, M.; Dürre, P.; Thauer, R.K. Energy conservation associated with ethanol formation from H_2 and CO_2 in *Clostridium autoethanogenum* involving electron bifurcation. *J. Bacteriol.* **2015**, *197*, 2965–2980. [CrossRef]
42. Nagarajan, H.; Sahin, M.; Nogales, J.; Latif, H.; Lovley, D.R.; Ebrahim, A.; Zengler, K. Characterizing acetogenic metabolism using a genome-scale metabolic reconstruction of *Clostridium ljungdahlii*. *Microb. Cell Fact.* **2013**, *12*, 118. [CrossRef]
43. Valgepea, K.; de Souza Pinto Lemgruber, R.; Meaghan, K.; Palfreyman, R.W.; Abdalla, T.; Heijstra, B.D.; Behrendorff, J.B.; Tappel, R.; Köpke, M.; Simpson, S.D.; et al. Maintenance of ATP homeostasis triggers metabolic shifts in gas-fermenting acetogens. *Cell Syst.* **2017**, *4*, 505–515. [CrossRef]
44. Aklujkar, M.; Leang, C.; Shrestha, P.M.; Shrestha, M.; Lovley, D.R. Transcriptomic profiles of *Clostridium ljungdahlii* during lithotrophic growth with syngas or H_2 and CO_2 compared to organotrophic growth with fructose. *Sci. Rep.* **2017**, *7*, 13135. [CrossRef]
45. Hermann, M.; Teleki, A.; Weitz, S.; Niess, A.; Freund, A.; Bengelsdorf, F.R.; Takors, R. Electron availability in CO_2, CO and H_2 mixtures constrains flux distribution, energy management and product formation in *Clostridium ljungdahlii*. *Microb. Biotechnol.* **2020**, *13*, 1831–1846. [CrossRef]
46. Fast, A.G.; Schmidt, E.D.; Jones, S.W.; Tracy, B.P. Acetogenic mixotrophy: Novel options for yield improvement in biofuels and biochemicals production. *Curr. Opin. Biotechnol.* **2015**, *33*, 60–72. [CrossRef]
47. Braun, K.; Gottschalk, G. Effect of molecular hydrogen and carbon dioxide on chemo-organotrophic growth of *Acetobacterium woodii* and *Clostridium aceticum*. *Arch. Microbiol.* **1981**, *128*, 294–298. [CrossRef] [PubMed]
48. Dahle, M.L.; Papoutsakis, E.T.; Antoniewicz, M.R. 13C-metabolic flux analysis of *Clostridium ljungdahlii* illuminates its core metabolism under mixotrophic culture conditions. *Metab. Eng.* **2022**, *72*, 161–170. [CrossRef] [PubMed]
49. Vees, C.A.; Herwig, C.; Pflügl, S. Mixotrophic co-utilization of glucose and carbon monoxide boosts ethanol and butanol productivity of continuous *Clostridium carboxidivorans* cultures. *Bioresour. Technol.* **2022**, *353*, 127138. [CrossRef] [PubMed]
50. Harahap, B.M.; Ahring, B.K. Acetate production from syngas produced from lignocellulosic biomass materials along with gaseous fermentation of the syngas: A review. *Microorganisms* **2023**, *11*, 995. [CrossRef]
51. Haas, T.; Krause, R.; Weber, R.; Demler, M.; Schmid, G. Technical photosynthesis involving CO_2 electrolysis and fermentation. *Nat. Catal.* **2018**, *1*, 32–39. [CrossRef]
52. Hortsch, R.; Corvo, P. The biorefinery concept: Producing cellulosic ethanol from agricultural residues. *Chem. Ing. Tech.* **2020**, *92*, 1803–1809. [CrossRef]
53. Alawad, I.; Ibrahim, H. Pretreatment of agricultural lignocellulosic biomass for fermentable sugar: Opportunities, challenges, and future trends. *Biomass Conv. Bioref.* **2024**, *14*, 6155–6183. [CrossRef]
54. Mann, M.; Munch, G.; Regestein, L.; Rehmann, L. Cultivation atrategies of *Clostridium autoethanogenum* on xylose and carbon monoxide combination. *ACS Sustain. Chem. Eng.* **2020**, *8*, 2632–2639. [CrossRef]
55. Oppelt, A.; Rückel, A.; Rupp, M.; Weuster-Botz, D. Mixotrophic syngas conversion enables the production of meso-2,3-butanediol with *Clostridium autoethanogenum*. *Fermentation* **2024**, *10*, 102. [CrossRef]
56. Zhao, Z.; Xian, M.; Liu, M.; Zhao, G. Biochemical routes for uptake and conversion of xylose by microorganisms. *Biotechnol. Biofuels* **2020**, *13*, 21. [CrossRef]
57. Jagtap, S.S.; Rao, C.V. Microbial conversion of xylose into useful bioproducts. *Appl. Microbiol. Biotechnol.* **2018**, *102*, 9015–9036. [CrossRef] [PubMed]
58. Jeffries, T.W. Utilization of xylose by bacteria, yeasts, and fungi. *Adv. Biochem. Eng. Biotechnol.* **1983**, *27*, 1–32. [CrossRef] [PubMed]
59. Lee, J.W.; Yook, S.; Koh, H.; Rao, C.V.; Jin, Y.-S. Engineering xylose metabolism in yeasts to produce biofuels and chemicals. *Curr. Opin. Biotechnol.* **2021**, *67*, 15–25. [CrossRef] [PubMed]

60. Doll, K.; Rückel, A.; Kämpf, P.; Wende, M.; Weuster-Botz, D. Two stirred-tank bioreactors in series enable continuous production of alcohols from carbon monoxide with *Clostridium carboxidivorans*. *Bioprocess Biosyst. Eng.* **2018**, *41*, 1403–1416. [CrossRef]
61. Iwakura, Y.; Iwata, K.; Matsuo, S.; Tohara, A. Synthesis of optically active poly(L-α-hydroxyisovalerate) and poly(L-α-hydroxyisocaproate). *Makromol. Chem.* **1971**, *146*, 21–32. [CrossRef]
62. Marubayashi, H.; Nojima, S. Crystallization and solid-state structure of poly(l-2-hydroxy-3-methylbutanoic acid). *Macromolecules* **2016**, *49*, 5538–5547. [CrossRef]
63. Tsuji, H.; Noda, S.; Kimura, T.; Sobue, T.; Arakawa, Y. Configurational molecular glue: One optically active polymer attracts two oppositely configured optically active polymers. *Sci. Rep.* **2017**, *7*, 45170. [CrossRef]
64. Cohen-Arazi, N.; Katzhendler, J.; Kolitz, M.; Domb, A.J. Preparation of new α-hydroxy acids derived from amino acids and their corresponding polyesters. *Macromolecules* **2008**, *41*, 7259–7263. [CrossRef]
65. Mahato, R.P.; Kumar, S.; Singh, P. Production of polyhydroxyalkanoates from renewable resources: A review on prospects, challenges and applications. *Arch. Microbiol.* **2023**, *205*, 172. [CrossRef]
66. Kalia, V.C.; Singh Patel, S.K.; Shanmugam, R.; Lee, J.-K. Polyhydroxyalkanoates: Trends and advances toward biotechnological applications. *Bioresour. Technol.* **2021**, *326*, 124737. [CrossRef]
67. Novák, L.; Loubiere, P. The metabolic network of *Lactococcus lactis*: Distribution of (14)C-labeled substrates between catabolic and anabolic pathways. *J. Bacteriol.* **2000**, *182*, 1136–1143. [CrossRef] [PubMed]
68. Wegmann, U.; O'Connell-Motherway, M.; Zomer, A.; Buist, G.; Shearman, C.; Canchaya, C.; Ventura, M.; Goesmann, A.; Gasson, M.J.; Kuipers, O.P.; et al. Complete genome sequence of the prototype lactic acid bacterium *Lactococcus lactis* subsp. *Lactococcus lactis* subsp. *cremoris* MG1363.. *J. Bacteriol.* **2007**, *189*, 3256–3270. [CrossRef]
69. Bolotin, A.; Wincker, P.; Mauger, S.; Jaillon, O.; Malarme, K.; Weissenbach, J.; Ehrlich, S.D.; Sorokin, A. The complete genome sequence of the lactic acid bacterium *Lactococcus lactis* ssp. lactis IL1403. *Genome Res.* **2001**, *11*, 731–753. [CrossRef] [PubMed]
70. Chambellon, E.; Rijnen, L.; Lorquet, F.; Gitton, C.; van Hylckama Vlieg, J.E.T.; Wouters, J.A.; Yvon, M. The D-2-hydroxyacid dehydrogenase incorrectly annotated PanE is the sole reduction system for branched-chain 2-keto acids in *Lactococcus lactis*. *J. Bacteriol.* **2009**, *191*, 873–881. [CrossRef]
71. Liew, F.; Henstra, A.M.; Köpke, M.; Winzer, K.; Simpson, S.D.; Minton, N.P. Metabolic engineering of *Clostridium autoethanogenum* for selective alcohol production. *Metab. Eng.* **2017**, *40*, 104–114. [CrossRef]
72. Köpke, M.; Gerth, M.L.; Maddock, D.J.; Mueller, A.P.; Liew, F.; Simpson, S.D.; Patrick, W.M. Reconstruction of an acetogenic 2,3-butanediol pathway involving a novel NADPH-dependent primary-secondary alcohol dehydrogenase. *Appl. Environ. Microbiol.* **2014**, *80*, 3394–3403. [CrossRef] [PubMed]
73. Cheong, S.; Clomburg, J.M.; Gonzalez, R. A synthetic pathway for the production of 2-hydroxyisovaleric acid in *Escherichia coli*. *J. Ind. Microbiol. Biotechnol.* **2018**, *45*, 579–588. [CrossRef] [PubMed]
74. Zheng, R.; Blanchard, J.S. Substrate specificity and kinetic isotope effect analysis of the *Eschericia coli* ketopantoate reductase. *Biochemistry* **2003**, *42*, 11289–11296. [CrossRef]
75. Wang, Q.; Jiang, W.; Cai, Y.; Tišma, M.; Baganz, F.; Shi, J.; Lye, G.J.; Xiang, W.; Hao, J. 2-Hydroxyisovalerate production by *Klebsiella pneumoniae*. *Enzym. Microb. Technol.* **2024**, *172*, 110330. [CrossRef]
76. Kracke, F.; Virdis, B.; Bernhardt, P.V.; Rabaey, K.; Krömer, J.O. Redox dependent metabolic shift in *Clostridium autoethanogenum* by extracellular electron supply. *Biotechnol. Biofuels* **2016**, *9*, 249. [CrossRef]
77. Allaart, M.T.; Diender, M.; Sousa, D.Z.; Kleerebezem, R. Overflow metabolism at the thermodynamic limit of life: How carboxydotrophic acetogens mitigate carbon monoxide toxicity. *Microb. Biotechnol.* **2023**, *16*, 697–705. [CrossRef] [PubMed]
78. Takors, R.; Kopf, M.; Mampel, J.; Bluemke, W.; Blombach, B.; Eikmanns, B.; Bengelsdorf, F.R.; Weuster-Botz, D.; Dürre, P. Using gas mixtures of CO, CO_2 and H_2 as microbial substrates: The do's and don'ts of successful technology transfer from laboratory to production scale. *Microb. Biotechnol.* **2018**, *11*, 606–625. [CrossRef] [PubMed]
79. Valgepea, K.; Souza Pinto Lemgruber, R.d.; Abdalla, T.; Binos, S.; Takemori, N.; Takemori, A.; Tanaka, Y.; Tappel, R.; Köpke, M.; Simpson, S.D.; et al. H_2 drives metabolic rearrangements in gas-fermenting *Clostridium autoethanogenum*. *Biotechnol. Biofuels* **2018**, *11*, 55. [CrossRef] [PubMed]